



CERN-EP-2022-071
29 March 2022

Photoproduction of low- p_T J/ψ from peripheral to central Pb–Pb collisions at 5.02 TeV

ALICE Collaboration*

Abstract

An excess of J/ψ yield at very low transverse momentum ($p_T < 0.3$ GeV/ c), originating from coherent photoproduction, is observed in peripheral and semicentral hadronic Pb–Pb collisions at a center-of-mass energy per nucleon pair of $\sqrt{s_{NN}} = 5.02$ TeV. The measurement is performed with the ALICE detector via the dimuon decay channel at forward rapidity ($2.5 < y < 4$). The nuclear modification factor at very low p_T and the coherent photoproduction cross section are measured as a function of centrality down to the 10% most central collisions. These results extend the previous study at $\sqrt{s_{NN}} = 2.76$ TeV, confirming the clear excess over hadronic production in the p_T range 0–0.3 GeV/ c and the centrality range 70–90%, and establishing an excess with a significance greater than 5σ also in the 50–70% and 30–50% centrality ranges. The results are compared with earlier measurements at $\sqrt{s_{NN}} = 2.76$ TeV and with different theoretical predictions aiming at describing how coherent photoproduction occurs in hadronic interactions with nuclear overlap.

arXiv:2204.10684v2 [nucl-ex] 4 Oct 2023

Diffraction photoproduction of J/ψ mesons in nucleus–nucleus collisions is sensitive to the nuclear gluon distributions at low Bjorken- x , in the range $x \sim 10^{-5}$ to 10^{-2} at LHC energies, where they are still poorly constrained [1–3]. This process was extensively studied in nuclear collisions with impact parameters larger than twice the nuclear radius, known as ultra-peripheral collisions (UPCs) [4–9]. In UPCs, hadronic interactions are strongly suppressed providing a clean experimental environment to study photon-induced processes.

Photonuclear reactions are produced by the strong electromagnetic field generated by ultra-relativistic ions, which can be treated as a flux of quasi-real photons. At leading order in perturbative quantum chromodynamics (pQCD), the photon fluctuates into a quark–antiquark pair (a color dipole) [10], which probes the gluon distribution of the target via the exchange of two gluons in a singlet color state, with the dipole finally recombining into a vector meson (VM) [11, 12]. The diffractive VM photoproduction on nuclei can be either coherent or incoherent. In the coherent interaction, the photon couples with the nucleus as a whole, leaving it intact. The produced VM is characterized by a very low average transverse momentum ($\langle p_T \rangle \approx 60$ MeV/ c). In incoherent photoproduction the photon couples to a single nucleon which leads to the breakup of the nucleus. In this case a VM with larger average transverse momentum ($\langle p_T \rangle \approx 500$ MeV/ c) is produced.

In nuclear collisions with impact parameters smaller than the sum of the radii of the colliding nuclei, production from hadronic interactions becomes the dominant contribution to the J/ψ yield. Hadroproduction of J/ψ mesons in Pb–Pb collisions is a long-standing probe of the quark–gluon plasma (QGP), a state of strongly-interacting matter characterized by quark and gluon degrees of freedom predicted by QCD to exist at high temperature and energy density. Charmonium production is affected by the QGP, and their measured yields [13–16] are explained as an interplay between suppression due to color screening [17] and recombination of charm quarks [18–20]. Finally, the charmonium yield can also be influenced by cold nuclear matter effects (CNM), which can be studied independently in p–Pb collisions [21–24].

The ALICE Collaboration reported the presence of an unexpectedly large J/ψ yield at very low p_T in peripheral Pb–Pb collisions at a center-of-mass energy per nucleon pair of $\sqrt{s_{NN}} = 2.76$ TeV [25], which could not be explained by any combination of suppression, regeneration, and CNM effects [26]. Coherent photoproduction of J/ψ in Pb–Pb collisions with nuclear overlap was proposed as a plausible mechanism to explain this observation [25]. A similar low- p_T J/ψ excess was later measured by the STAR Collaboration at RHIC in Au–Au collisions at $\sqrt{s_{NN}} = 200$ GeV and U–U collisions at $\sqrt{s_{NN}} = 193$ GeV [27]. The STAR measurement of the t -dependence (Mandelstam variable, $t \approx -p_T^2$ for large $\sqrt{s_{NN}}$) of the excess showed a strong similarity with the one measured in UPCs, also pointing to coherent photoproduction as the origin of the excess. Similar conclusions can be drawn from the recent measurement of the J/ψ yields at low p_T in Pb–Pb collisions at $\sqrt{s_{NN}} = 5.02$ TeV by the LHCb Collaboration [28]. In addition, dilepton pairs with characteristics compatible with photoproduction were observed in non-UPC heavy-ion collisions by the ATLAS, STAR, and ALICE experiments [29–31].

The concept of coherent photoproduction in a hadronic environment raises several theoretical challenges. For example, how can the coherence condition survive in the photon–nucleus interaction if the latter is broken up during the hadronic collision? Do only the (non-interacting) spectator nucleons participate in the coherent process? To what extent is the photon–nucleus cross section modified by target nucleons undergoing hadronic interactions and losing energy before the photoproduction occurs? How is the yield of the photoproduced J/ψ mesons, characterized by low transverse momenta, affected by interactions with the formed and fast-expanding QGP medium? The measurements mentioned above triggered novel theoretical developments [26, 32–36] based on calculations for UPCs in which the nuclear photoproduction cross section of a VM is usually computed as the product of a quasi-real photon flux with the photon–nucleus cross section corresponding to the $\gamma A \rightarrow VM + A$ interaction, where γ is the photon and A is the nucleus. For collisions with nuclear overlap, in all considered models, an effective photon flux is introduced to take into account the geometrical constraints of a given impact-parameter range. Depending on

the model, the photon-nucleus cross section is sometimes also modified to account for the effective size of nuclear fragments participating in the coherent process [32, 34]. Calculations from Ref. [34] highlight the interest of measuring the cross section (and additionally its transverse momentum dependence) of the J/ψ excess towards more central collisions in order to probe possible changes of the effective size of the coherently interacting volume. Additionally, it was suggested that the measurement of the J/ψ coherent photoproduction in UPCs and in peripheral collisions in the same rapidity range at forward rapidity can be used to extract the coherent photon-nucleus cross section in two different Bjorken- x regions, below 10^{-4} and above 10^{-2} at LHC energies [37].

In this Letter, the measurement of the J/ψ nuclear modification factor and the coherent photoproduction at low p_T at forward rapidity in Pb–Pb collisions at $\sqrt{s_{NN}} = 5.02$ TeV are presented as a function of collision centrality. The measurement uses a pp reference at the same energy that is described in Ref. [38]. The larger data set compared to the one at $\sqrt{s_{NN}} = 2.76$ TeV [25] allows for the first time the observation of a significant excess in the 50–70% and 30–50% centrality intervals. Assuming that the observed excess originates from coherent J/ψ photoproduction, the corresponding cross section is extracted as a function of the collision centrality. For centrality intervals where no significant excess could be measured, an upper limit on the cross section is reported.

The ALICE detector and its performance are described in detail in Refs. [39, 40]. In this analysis, the J/ψ production is measured at forward rapidity ($2.5 < y < 4$) and down to $p_T = 0$ in the dimuon decay channel with the forward muon spectrometer, consisting of a tracking system placed downstream of a front absorber of composite material, and a trigger system placed downstream of a muon filter made of iron. The interaction vertex is determined with the Silicon Pixel Detector (SPD), which consists of the two innermost layers of the Inner Tracking System in the central barrel. The first and second innermost layers cover the pseudorapidity ranges $|\eta| < 2$ and $|\eta| < 1.4$, respectively. The V0 detector, consisting of two scintillator hodoscopes placed on both sides of the interaction point and covering the pseudorapidity range $2.8 < \eta < 5.1$ and $-3.7 < \eta < -1.7$, is used for triggering, beam–gas background rejection and determination of the collision centrality, which is evaluated by fitting the signal amplitude distribution in the V0 as described in Ref. [41]. The Zero Degree Calorimeters (ZDCs) are placed on both sides of the interaction point along the beam direction at a distance of 112.5 m from it and measure the spectator protons and neutrons. The requirement of a minimum energy deposited in the two neutron calorimeters, corresponding to the expected signal from one spectator neutron, and the combined use of the V0 and ZDC timing information, suppresses the background induced by electromagnetic dissociation processes [42].

The data sample considered in this analysis, collected in 2015 and 2018, consists of events where two opposite sign muons are detected in the trigger system of the muon spectrometer, each with a p_T above the trigger threshold of 1 GeV/ c , in coincidence with a minimum-bias (MB) trigger. The latter is defined by the coincidence of a signal in both arrays of the V0 detector. Events are selected in the 0–90% centrality interval, where the MB trigger is fully efficient. The data sample used for this analysis amounts to 4×10^8 triggered Pb–Pb collisions, corresponding to an integrated luminosity of $756 \pm 19 \mu\text{b}^{-1}$ [43], where the uncertainty is systematic (the statistical one being negligible).

J/ψ candidates are formed by combining pairs of opposite-sign (OS) muon tracks reconstructed in the geometrical acceptance of the muon spectrometer ($-4 < \eta < -2.5$). The muon identification is ensured by requiring that each track reconstructed in the tracking chambers matches a track segment in the trigger system. The single-muon and dimuon selection criteria are the same as the ones used in previous analyses [14, 25]. The raw number of J/ψ is extracted in five centrality classes (0–10%, 10–30%, 30–50%, 50–70% and 70–90%) and two p_T ranges with the aim to study the coherent (0–0.3 GeV/ c) and the incoherent photoproduction (0.3–1 GeV/ c). The choice of the transverse momentum intervals takes into account the broadening of the reconstructed transverse momentum distribution of coherently and incoherently photoproduced J/ψ , mainly due to multiple scattering in the front absorber. The raw

yield is also extracted in eight p_T intervals up to 8 GeV/ c in order to estimate the hadronic contribution as explained below. The signal extraction is performed by fitting the invariant mass distribution of the OS dimuons using various combinations of functional forms for the signal and background shapes as discussed in the following. The raw J/ψ yield and its statistical uncertainty is then determined as the average of all obtained yield values and corresponding statistical uncertainties, respectively, while the associated systematic uncertainty is taken as the standard deviation of the results. The signal is modeled through an extended Crystal Ball function or a pseudo-Gaussian with a mass-dependent width [44]. The non-Gaussian tails were fixed to the values obtained by fitting either a large sample in pp collisions at $\sqrt{s} = 13$ TeV [45] or MC simulations where the hadroproduced J/ψ signal is embedded into real events in order to account for detector occupancy effects. In the p_T ranges 0–0.3 GeV/ c and 0.3–1 GeV/ c , additional sets of tails are obtained from MC simulations that use as input coherently and incoherently photoproduced J/ψ from the STARlight MC generator [46]. The underlying continuum is described with either a variable-width Gaussian or the ratio of second and third order polynomials [44, 47].

The nuclear modification factor in the centrality interval i is defined as

$$R_{AA}^i(p_T) = \frac{N_{J/\psi}^i(p_T)}{\text{BR}_{J/\psi \rightarrow \mu^+\mu^-} \times N_{\text{MB}}^i \times A\varepsilon^{i,h}(p_T) \times \langle T_{AA}^i \rangle \times \sigma_{\text{pp}}(p_T)}, \quad (1)$$

where $N_{J/\psi}^i$ are the measured raw yields, $A\varepsilon^{i,h}$ is the detector acceptance and efficiency (assuming unpolarized hadroproduction), $\text{BR}_{J/\psi \rightarrow \mu^+\mu^-}$ is the branching ratio to muon pairs [48], N_{MB}^i is the equivalent number of MB events, $\langle T_{AA}^i \rangle$ is the average nuclear overlap function, and σ_{pp} is the measured J/ψ cross section in pp collisions at the same center-of-mass energy [38].

The $A\varepsilon$ values are estimated with MC simulations where the J/ψ input p_T and y distributions are adjusted to data, and separately tuned for each centrality class using an iterative procedure. The time-dependent status of the electronics channels for the tracking chambers, as well as misalignment of the detector elements, were taken into account. The efficiency of the trigger chambers was determined from data and used in the simulations. The systematic uncertainty on the $A\varepsilon$ value derives from the uncertainty on the MC input p_T and y distributions and on the tracking, trigger and matching efficiency. The former was evaluated by varying the input shapes tuned on data within the statistical uncertainty and by taking into account the correlations between the p_T and y distributions. Assuming that the uncertainty related to the correlation does not depend on the collision system and energy, this uncertainty was estimated using a large pp sample [45], by comparing the $A\varepsilon$ values obtained from p_T (y) dependent input shapes extracted in narrower y (p_T) intervals with those obtained using the corresponding shapes from the full y and p_T range. The remaining uncertainties on the $A\varepsilon$ were determined following the procedure described in detail in Ref. [14].

The normalization to MB events, N_{MB}^i , is computed as the product of the number of dimuon-triggered events and the inverse of the probability of having a dimuon trigger in a MB event, for the relevant centrality class i . This probability can be obtained with two methods, as explained in Ref. [47]; the difference is taken as the systematic uncertainty.

The average nuclear overlap function $\langle T_{AA} \rangle$ and number of participants $\langle N_{\text{part}} \rangle$ (i.e. the number of nucleons in the nuclei undergoing inelastic scattering) are obtained from a Glauber model fit of the V0 amplitude [49, 50]. The uncertainty on the value of the V0 signal amplitude corresponding to the most central 90% of the total hadronic Pb–Pb cross section is $\pm 1\%$. This uncertainty is propagated into the definition of the centrality intervals as explained in Ref. [47].

The systematic uncertainties on the R_{AA} measurement as a function of centrality are summarized in Table 1.

Figure 1 shows the R_{AA} as a function of the number of participants $\langle N_{\text{part}} \rangle$. The relationship between

Table 1: Systematic uncertainties (in percent) on the R_{AA} measurement for different J/ψ p_T intervals. Ranges correspond to the range of values in different centrality classes, whereas the values marked with an asterisk are independent of centrality.

p_T	0–0.3 GeV/c	0.3–1 GeV/c	1–2 GeV/c
Signal extraction	1.8–3.7	1.5–3.4	2.4–3.4
MC input	2.5		
Tracking eff.	0–1 + 3*		
Trigger eff.	0–1 + 2.8*	0–1 + 2.0*	0–1 + 1.5*
Matching eff.	1*		
N_{MB}	0.3*		
$\langle T_{AA} \rangle$	0.7–2.4		
Centrality limits	0.2–7		
pp cross section	5.8*	5.4*	5.1*

$\langle N_{part} \rangle$ and centrality is provided in Table 2. The J/ψ R_{AA} for $p_T < 0.3$ GeV/c (where coherent photoproduction would be highest) and $0.3 < p_T < 1.0$ GeV/c (where incoherent photoproduction could contribute) is compared with the R_{AA} for $1.0 < p_T < 2.0$ GeV/c (where hadroproduction dominates). The J/ψ R_{AA} in the p_T interval 0–0.3 GeV/c is significantly larger than the R_{AA} at larger transverse momenta, except for the most central events. It reaches a value of about 10 for the most peripheral events. This large increase is similar to the one of about a factor 7 measured at a lower center-of-mass energy [25]. The measurement in the interval 0.3–1 GeV/c is compatible with the one in 1–2 GeV/c except for the most peripheral events, where it is larger by roughly 2 standard deviations (σ). Further studies of the kinematic distribution of this signal could confirm the origin from incoherent photoproduction processes. Data are compared with a model [26] that includes initial J/ψ production, J/ψ regeneration, and a J/ψ photoproduction component for $p_T < 0.3$ GeV/c. The uncertainty band of the theoretical predictions is mainly due to the variation of the shadowing factor. QGP effects on the photoproduced J/ψ are taken into account as well. The theoretical predictions well describe data in the p_T and centrality ranges considered.

The excess with respect to the expected hadronic production was quantified with the same procedure as used in Ref. [25]. For each centrality class, the hadronic J/ψ yield ($\frac{dN_{AA}^{i,h}}{dp_T}$) as a function of p_T is parameterized with:

$$\frac{dN_{AA}^{i,h}}{dp_T}(p_T) = \mathcal{N} \times \frac{d\sigma_{pp}^h}{dp_T}(p_T) \times R_{AA}^{i,h}(p_T) \times A\epsilon^{i,h}(p_T). \quad (2)$$

The normalization factor \mathcal{N} is defined in such a way that the integral of the function in the p_T interval 1–8 GeV/c is equal to the measured number of J/ψ in the same interval, which is dominated by hadroproduction. The $\frac{d\sigma_{pp}^h}{dp_T}$ is taken from a fit to the pp cross section measured by ALICE at $\sqrt{s} = 5.02$ TeV [38] with either a power law function [51] or a Lévy–Tsallis function [52, 53]. $R_{AA}^{i,h}$ is a fit to the measured nuclear modification factor as a function of p_T for the same centrality classes as presented above. For the central to semicentral intervals (0–50%) a Woods–Saxon like function [25] is used, with the parameter p_T^0 defining the 50% crossing point fixed to various values related to the J/ψ mass and average transverse momentum $\langle p_T \rangle$. This function was chosen since it can describe the transport model predictions for J/ψ production in heavy-ion collisions [54, 55]. For the most peripheral intervals (50–90%), where the recombination effects in the QGP are expected to be smaller, a linear and a constant function are used. The fit is performed in two p_T intervals 0.65–15 GeV/c and 1–15 GeV/c, where the hadroproduction is the main contribution, and then extrapolated to $p_T = 0$. For the Woods–Saxon function, the quality of the low- p_T extrapolation is assessed by verifying that the functional form reproduces the measured R_{AA} in the most central events where the hadronic contribution is dominant. Finally, $A\epsilon^{i,h}$ is a fit to the hadronic J/ψ acceptance and efficiency for the centrality class i , using a ratio of two Lévy–Tsallis functions. In

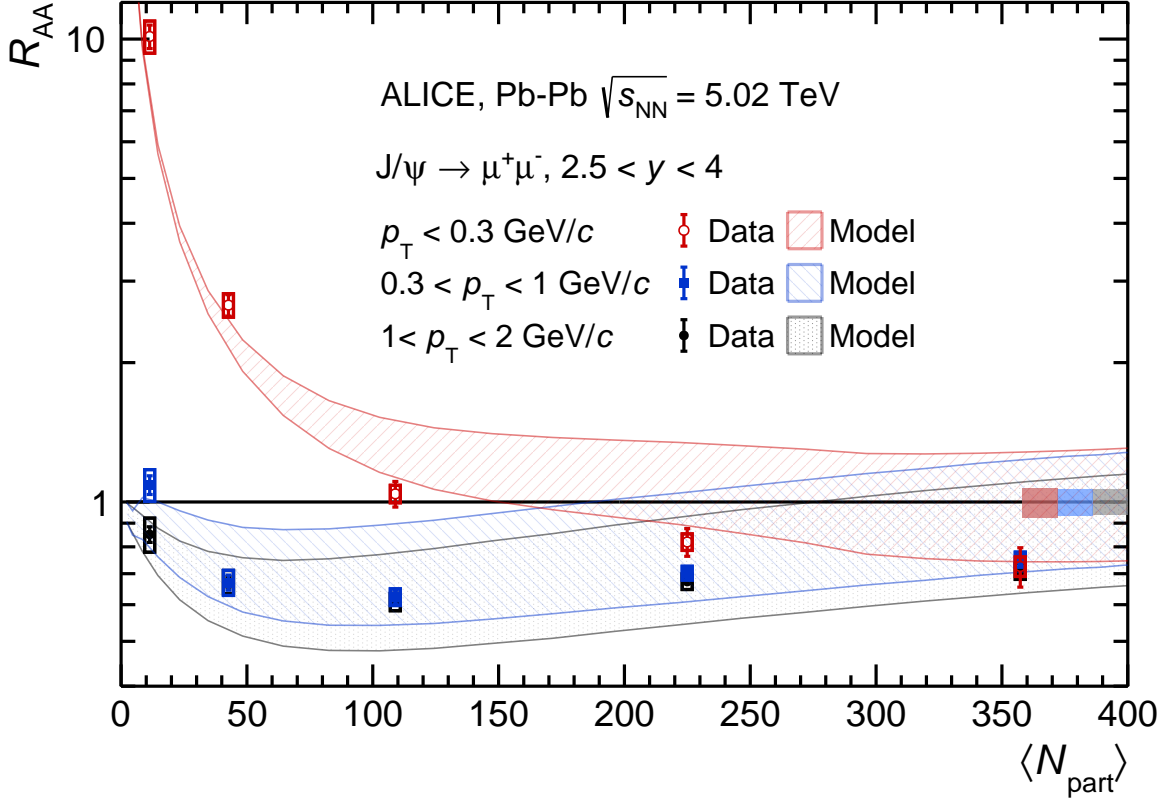


Figure 1: J/ψ nuclear modification factor as a function of $\langle N_{\text{part}} \rangle$ measured in the rapidity range $2.5 < y < 4$ for three transverse momentum intervals. The vertical bars are the statistical uncertainties and the uncorrelated systematic uncertainties are represented as boxes. The centrality-correlated systematic uncertainties are shown as filled boxes at unity. Data are compared with predictions from Ref. [26], shown as bands.

order not to double-count the uncertainties on the pp cross section and on the Pb–Pb $A\mathcal{E}$, those were disregarded in the fit to the R_{AA} . Each combination of different parametrizations and fit ranges results in a different hadronic J/ψ distribution as a function of p_T , which is then integrated in the p_T interval 0–0.3 GeV/c. The final numbers of expected hadronic J/ψ , defined as the averages of the obtained values, are listed in Table 2 (fourth column) together with the raw measured numbers of J/ψ (third column). For the expected hadronic yields, the statistical uncertainty comes from the statistical uncertainty on \mathcal{N} , which derives from the statistical uncertainty on the J/ψ raw yield in 1–8 GeV/c. The systematic uncertainty of the expected yields is taken as the quadratic sum of the standard deviation of the results obtained using different parametrizations and fit ranges, and the average of the individual systematic uncertainties for the variations (including contributions from all factors in Eq. 2).

The estimated number of hadroproduced J/ψ is subtracted from the measured raw signal to obtain the number of J/ψ in excess (fifth column of Table 2). The measured number of J/ψ exceeds the hadronic production by 24σ in the 70–90% centrality class, 16σ in 50–70%, 5.6σ in 30–50% and 1.4σ in 10–30%. A 95% confidence interval when combining all uncertainties is provided in the centrality class 0–10% where no significant excess is observed within the current experimental uncertainties.

Assuming that the underlying process for the J/ψ excess is photoproduction, the number of coherently photoproduced J/ψ in $0 < p_T < 0.3$ GeV/c can be extracted after correcting the excess yield for the fractions of J/ψ from incoherent photoproduction (f_1) and from the decay of coherently photoproduced

Table 2: Average number of participants, measured number of J/ψ , estimated number of hadronic J/ψ , difference between these two quantities and resulting J/ψ cross section for coherent photoproduction in the transverse momentum interval 0–0.3 GeV/ c for the listed centrality classes. The first quoted uncertainty corresponds to the statistical uncertainty, the second to the centrality uncorrelated systematic uncertainty; in addition, a correlated systematic uncertainty of 6.6% applies to the cross section in all centrality classes. For the 0–10% centrality class, the quoted values correspond to a 95% confidence level interval.

Centrality class	$\langle N_{\text{part}} \rangle$	$N_{\text{raw}}^{J/\psi}$	$N_{\text{hadro}}^{J/\psi}$	$N_{\text{excess}}^{J/\psi}$	$d\sigma_{\text{coh}}^{J/\psi}/dy$ (μb)
0–10%	357.3 ± 0.8	$8351 \pm 762 \pm 312$	$8713 \pm 86 \pm 873$	< 2406 (95% CL)	< 230 (95% CL)
10–30%	225.0 ± 1.2	$9624 \pm 571 \pm 278$	$8274 \pm 60 \pm 742$	$1350 \pm 574 \pm 792$	$145 \pm 62 \pm 85$
30–50%	109.0 ± 1.1	$4280 \pm 225 \pm 105$	$2562 \pm 23 \pm 178$	$1718 \pm 226 \pm 207$	$179 \pm 24 \pm 22$
50–70%	42.7 ∓ 0.7	$2763 \pm 98 \pm 68$	$674 \pm 8 \pm 40$	$2089 \pm 98 \pm 79$	$216 \pm 10 \pm 12$
70–90%	11.3 ± 0.2	$1758 \pm 57 \pm 32$	$138 \pm 3 \pm 9$	$1620 \pm 57 \pm 33$	$167 \pm 6 \pm 12$

Table 3: Systematic uncertainties on the coherent J/ψ cross section (notation is the same as in Table 1).

Source	Value (%)
Branching Ratio	0.5*
$N_{\text{excess}}^{J/\psi}$	2–58.7
f_I	2.9*
f_D	1.1*
Tracking eff.	0–0.5 + 3*
Trigger eff.	0–0.5 + 3.6*
Matching eff.	1*
MC input	0.1*
p_T selection	2*
Centrality limits	0.2–7
\mathcal{L}_{int}	2.5*

$\psi(2S)$ (f_D) as described in Ref. [7]. Those fractions were measured in UPC collisions at the same center-of-mass energy, although in a slightly different p_T interval, $p_T < 0.25$ GeV/ c [7]. They were therefore recomputed for $p_T < 0.3$ GeV/ c . The corresponding values and systematic uncertainties are $f_I = 0.089 \pm 0.034$ and $f_D = 0.066 \pm 0.013$. In the following it was assumed that these fractions are the same in UPC and hadronic collisions and that they do not depend significantly on the collision centrality. The first assumption seems realistic for f_D , although f_I might vary if the coherence is incomplete in the presence of hadronic interactions.

Finally, the cross section is obtained by correcting the excess yield for the branching ratio to OS dimuons, for the $A\mathcal{E}$ factor estimated by means of STARlight [46] simulations embedded into data for each centrality class, taking into account that the coherently photoproduced J/ψ mesons are expected to be transversely polarized, and by normalizing to the integrated luminosity and the width of the rapidity range. The systematic uncertainties are summarized in Table 3. The uncertainties on the number of excess J/ψ are discussed above. The contributions from the $A\mathcal{E}$ are the same as in Table 1, except for the one on the STARlight MC input, which is obtained as described in Ref. [7]. An additional systematic uncertainty of 2% due to the transverse momentum resolution was estimated by comparing the $A\mathcal{E}$ obtained with or without the p_T selection at 0.3 GeV/ c . The systematic uncertainty on the luminosity mainly originates from the uncertainty of the reference V0 trigger cross section measured with van der Meer scans [43]. The uncertainties on f_I and f_D are estimated as described in Ref. [7].

The coherent J/ψ photoproduction cross section at $\sqrt{s_{\text{NN}}} = 5.02$ TeV as a function of $\langle N_{\text{part}} \rangle$ is shown in Figure 2. Empty boxes correspond to the uncorrelated systematic uncertainties. The correlated sys-

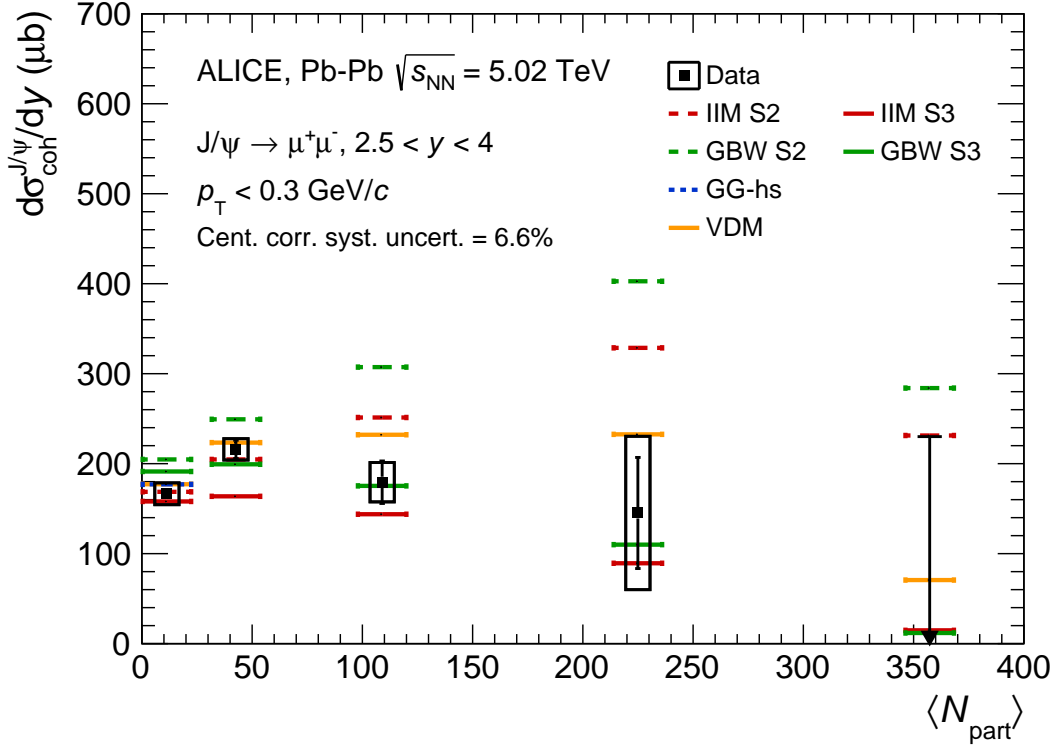


Figure 2: J/ψ coherent photoproduction cross section as a function of $\langle N_{\text{part}} \rangle$ at forward rapidity in Pb–Pb collisions at $\sqrt{s_{\text{NN}}} = 5.02$ TeV. The vertical bars are the statistical uncertainties and the uncorrelated systematic uncertainties are represented as boxes. The centrality correlated systematic uncertainties are quoted in the legend. Results are compared with theoretical calculations from Ref. [33] (GG-hs), Ref. [32] (IIM S2 and S3, and GBW S2 and S3) and from Ref. [35] with updated Glauber calculations from Ref. [56] (VDM). The figure shows the integral of the cross section measurement as well as the corresponding theoretical model values in each centrality interval. Note that the most central bin, where only an upper limit is given, is half the size of the other intervals. Therefore, to evaluate the centrality dependence of J/ψ coherent photoproduction, both data and theory have to be multiplied by a factor of two.

tematic uncertainty amounts to 6.6%, independent of centrality, and is quoted in the legend.

The result is compared with theoretical calculations that use an effective description based on UPC color dipole models. The GG-hs calculations [33] are based on models representing subnucleonic degrees of freedom as hot spots, whose number increases with increasing photon-target center of mass energy. The calculation is extended from protonic to nuclear targets using Glauber–Gribov formalism (GG) [33]. The photon flux is estimated in the same way as in the UPC case, but the integral is limited to the impact parameter range of the selected centrality class. The calculation from Ref. [56] is based on a vector dominance model, in which the photon fluctuates into a vector meson component that propagates through the nucleus and fragments into an on-shell vector meson. In this model, which will be referred to as VDM in the following, the photon flux is modified with respect to the one used in UPC calculations by considering only the photons that reach the geometrical region of the target nucleus outside of the overlap region. In the GBW calculation, the light cone color dipole formalism is used, while the IIM calculation is based on the Color Glass Condensate approach [32]. The GBW and IIM calculations provide two scenarios. In the first one (called S2 in Ref. [32]), the photon flux is modified in a similar way as for the VDM model. However, in contrast with the latter, an effective area is used in building the flux, which disregards the region of nuclear overlap. This prevents the flux and the resulting cross section from being progressively reduced towards more central collisions. In the second scenario (S3),

an additional modification of the photon-nucleus cross section is introduced, in which the overlap region between the two nuclei is assumed not to contribute to coherent photoproduction resulting in significant reduction of the photoproduction cross sections towards more central collisions.

The hot-spot model prediction (GG-hs) is only available for the most peripheral centrality interval (70–90%) where the calculation is compatible with data. The other models provide predictions for all centrality intervals. The VDM model predicts a mild increase of the cross section in peripheral events, a flat evolution in semi-central events, and a decrease of the cross section in the most central events, in fair agreement with data. Notice that the figure shows the integral of the cross section in each centrality interval and the most central interval is half the size of the others. If one accounts for the interval width, the predictions for the most central interval would be twice as large, resulting in a rather mild decrease of the cross section with centrality. This model uses an optical Glauber model to describe the collision centrality, but a similar agreement with data can be obtained with a simplified relation between impact parameter and centrality [35]. The IIM and GBW models with unmodified photon-nucleus cross section (S2) predict a steady increase of the J/ψ coherent photoproduction cross section with centrality, once the width of the centrality intervals is properly accounted for. In data, this increasing trend is only observed for the two most peripheral intervals. In this scenario, the GBW model overestimates the data in all centrality intervals. The IIM model is in agreement with data in the first two centrality intervals, while it starts to deviate from the data by 2.1σ in the 30–50% centrality interval. The S3 version of the GBW and IIM models [32] excluding the nuclear overlap region from the photon-nucleus cross section calculation predicts a decrease of the cross section from semicentral to central events (similar to the one of Ref. [56], which, however, requires only a modification of the photon flux), and is compatible with the data in the full centrality range considering the current uncertainties. Since the transverse momentum of the coherently photoproduced vector meson is of the order of the inverse of the target size, the interaction occurring with the remaining nucleus fragment outside the overlap area would result in a larger average p_T and a wider p_T distribution for the photoproduced J/ψ . A measurement of the J/ψ p_T distribution at low p_T is therefore needed to clarify what is the underlying mechanism leading to the observed distribution as a function of centrality.

The models described here provided predictions also for the measurement at $\sqrt{s_{NN}} = 2.76$ TeV [25]. The corresponding figure can be found in the Appendix A. The ratio of the measurements at $\sqrt{s_{NN}} = 5.02$ TeV and $\sqrt{s_{NN}} = 2.76$ TeV [25] is shown in Fig. 3. In the ratio, only the systematic uncertainty on the branching ratio cancels out. The centrality uncorrelated (correlated) systematic uncertainties in Table 3 are represented as open (filled) boxes in Fig. 3. The centrality correlated uncertainties are mainly due to the uncertainty on f_I and f_D , which were asymmetric in the estimation performed at $\sqrt{s_{NN}} = 2.76$ TeV. The cross section increase with the center-of-mass energy does not depend significantly on the centrality. Figure 3 shows that the hot-spot model tends to underpredict the increase of the cross section with the center-of-mass energy in peripheral hadronic interactions, while the other models are in fair agreement with the measured ratio in all centrality ranges within the large uncertainties. For the IIM and GBW models no distinction is done in this case between the scenarios with or without modification of the photon-nucleus cross section since their energy dependence is exactly the same.

In summary, this Letter reports the measurement of J/ψ production at very low p_T as a function of centrality in hadronic Pb–Pb collisions at $\sqrt{s_{NN}} = 5.02$ TeV at forward rapidity. The nuclear modification factor R_{AA} shows a large enhancement of the J/ψ yield for $p_T < 0.3$ GeV/ c with respect to expectations from hadronic production. This excess, which was previously seen in more peripheral collisions, is now confirmed to be present for most of the total hadronic cross section, including in collisions with a large nuclear overlap, down to at least a level of 30% in centrality. The enhancement has a significance of 24σ in the 70–90% centrality class, 16σ in 50–70% and 5.6σ in the centrality class 30–50%. The reported observation extends previous measurements performed by the ALICE, LHCb and STAR Collaborations, supporting coherent photoproduction in hadronic collisions as the underlying mechanism. Based on this

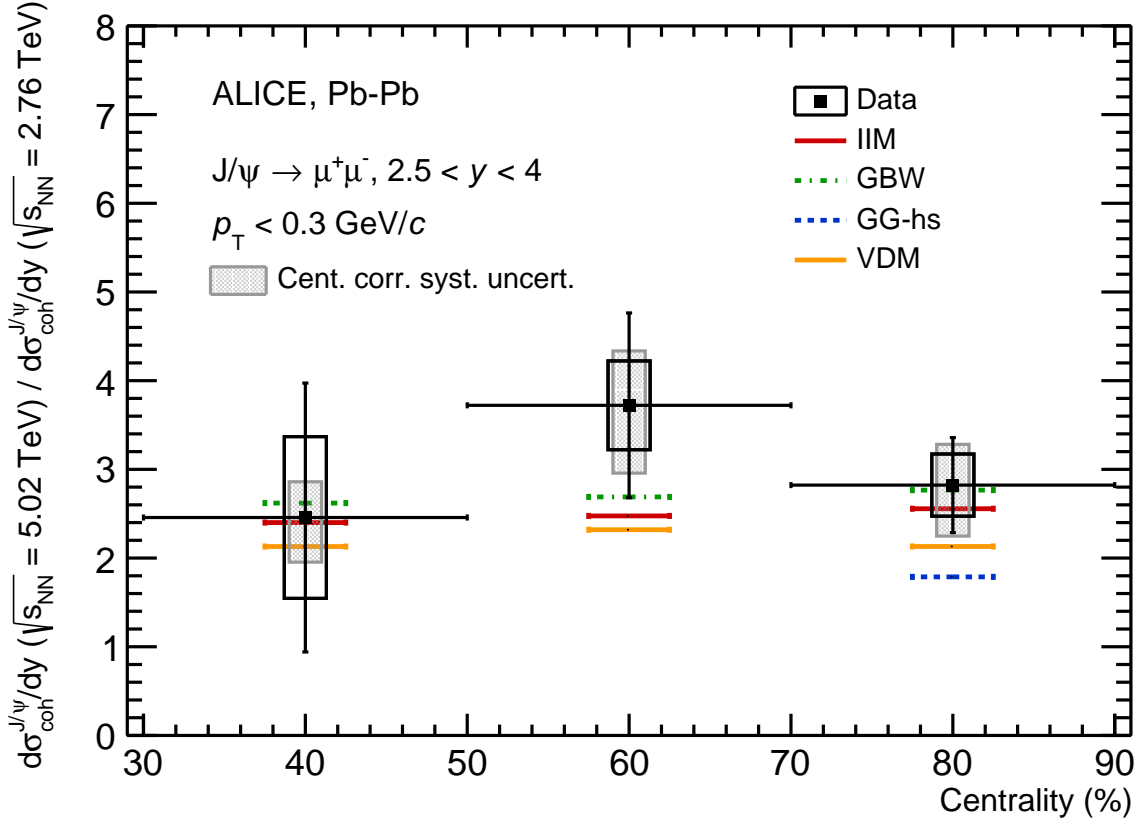


Figure 3: J/ψ coherent photoproduction cross section ratio for two different energies ($\sqrt{s_{NN}} = 5.02$ TeV over $\sqrt{s_{NN}} = 2.76$ TeV) as a function of centrality. The data at $\sqrt{s_{NN}} = 2.76$ TeV are taken from Ref. [25]. The vertical lines are the statistical uncertainties while the open (filled) boxes are the centrality uncorrelated (correlated) systematic uncertainties. Results are compared with theoretical calculations from Ref. [33] (GG-hs), Ref. [32] (IIM and GBW) and from Ref. [35] with updated Glauber calculations from Ref. [56] (VDM).

assumption, the corresponding cross section is extracted for the centrality classes 10–30%, 30–50%, 50–70% and 70–90% while an upper limit is given for 0–10%. The ratio of coherent photoproduction cross sections for $\sqrt{s_{NN}} = 5.02$ TeV over $\sqrt{s_{NN}} = 2.76$ TeV is extracted as a function of centrality and shows a flat dependence on centrality within uncertainties. A set of theoretical calculations successfully used to describe coherent photoproduction in UPC, and modified to account for geometrical constraints on the photon flux in the selected centrality classes, is compared with the measurement. The cross section as a function of centrality is well described by two models, one implementing a modification of the photon flux only [56], and the other requiring an additional modification of the photon-nucleus cross section [32]. Additional measurements of the p_T -differential photoproduction cross section as a function of centrality and further comparison with models using different photoproduction scenarios would help to clarify the effect of the disruption of the nucleus and nucleons by hadronic interactions on the coherence condition of vector meson photoproduction.

Acknowledgements

The ALICE Collaboration would like to thank all its engineers and technicians for their invaluable contributions to the construction of the experiment and the CERN accelerator teams for the outstanding performance of the LHC complex. The ALICE Collaboration gratefully acknowledges the resources and

support provided by all Grid centres and the Worldwide LHC Computing Grid (WLCG) collaboration. The ALICE Collaboration acknowledges the following funding agencies for their support in building and running the ALICE detector: A. I. Alikhanyan National Science Laboratory (Yerevan Physics Institute) Foundation (ANSL), State Committee of Science and World Federation of Scientists (WFS), Armenia; Austrian Academy of Sciences, Austrian Science Fund (FWF): [M 2467-N36] and Nationalstiftung für Forschung, Technologie und Entwicklung, Austria; Ministry of Communications and High Technologies, National Nuclear Research Center, Azerbaijan; Conselho Nacional de Desenvolvimento Científico e Tecnológico (CNPq), Financiadora de Estudos e Projetos (Finep), Fundação de Amparo à Pesquisa do Estado de São Paulo (FAPESP) and Universidade Federal do Rio Grande do Sul (UFRGS), Brazil; Bulgarian Ministry of Education and Science, within the National Roadmap for Research Infrastructures 2020-2027 (object CERN), Bulgaria; Ministry of Education of China (MOEC), Ministry of Science & Technology of China (MSTC) and National Natural Science Foundation of China (NSFC), China; Ministry of Science and Education and Croatian Science Foundation, Croatia; Centro de Aplicaciones Tecnológicas y Desarrollo Nuclear (CEADEN), Cubaenergía, Cuba; Ministry of Education, Youth and Sports of the Czech Republic, Czech Republic; The Danish Council for Independent Research | Natural Sciences, the VILLUM FONDEN and Danish National Research Foundation (DNRF), Denmark; Helsinki Institute of Physics (HIP), Finland; Commissariat à l’Energie Atomique (CEA) and Institut National de Physique Nucléaire et de Physique des Particules (IN2P3) and Centre National de la Recherche Scientifique (CNRS), France; Bundesministerium für Bildung und Forschung (BMBF) and GSI Helmholtzzentrum für Schwerionenforschung GmbH, Germany; General Secretariat for Research and Technology, Ministry of Education, Research and Religions, Greece; National Research, Development and Innovation Office, Hungary; Department of Atomic Energy Government of India (DAE), Department of Science and Technology, Government of India (DST), University Grants Commission, Government of India (UGC) and Council of Scientific and Industrial Research (CSIR), India; National Research and Innovation Agency - BRIN, Indonesia; Istituto Nazionale di Fisica Nucleare (INFN), Italy; Japanese Ministry of Education, Culture, Sports, Science and Technology (MEXT) and Japan Society for the Promotion of Science (JSPS) KAKENHI, Japan; Consejo Nacional de Ciencia (CONACYT) y Tecnología, through Fondo de Cooperación Internacional en Ciencia y Tecnología (FONCICYT) and Dirección General de Asuntos del Personal Académico (DGAPA), Mexico; Nederlandse Organisatie voor Wetenschappelijk Onderzoek (NWO), Netherlands; The Research Council of Norway, Norway; Commission on Science and Technology for Sustainable Development in the South (COMSATS), Pakistan; Pontificia Universidad Católica del Perú, Peru; Ministry of Education and Science, National Science Centre and WUT ID-UB, Poland; Korea Institute of Science and Technology Information and National Research Foundation of Korea (NRF), Republic of Korea; Ministry of Education and Scientific Research, Institute of Atomic Physics, Ministry of Research and Innovation and Institute of Atomic Physics and University Politehnica of Bucharest, Romania; Ministry of Education, Science, Research and Sport of the Slovak Republic, Slovakia; National Research Foundation of South Africa, South Africa; Swedish Research Council (VR) and Knut & Alice Wallenberg Foundation (KAW), Sweden; European Organization for Nuclear Research, Switzerland; Suranaree University of Technology (SUT), National Science and Technology Development Agency (NSTDA) and National Science, Research and Innovation Fund (NSRF via PMU-B B05F650021), Thailand; Turkish Energy, Nuclear and Mineral Research Agency (TENMAK), Turkey; National Academy of Sciences of Ukraine, Ukraine; Science and Technology Facilities Council (STFC), United Kingdom; National Science Foundation of the United States of America (NSF) and United States Department of Energy, Office of Nuclear Physics (DOE NP), United States of America. In addition, individual groups or members have received support from: Marie Skłodowska Curie, Strong 2020 - Horizon 2020, European Research Council (grant nos. 824093, 896850, 950692), European Union; Academy of Finland (Center of Excellence in Quark Matter) (grant nos. 346327, 346328), Finland; Programa de Apoyos para la Superación del Personal Académico, UNAM, Mexico;

References

- [1] K. J. Eskola, P. Paakkinen, H. Paukkunen, and C. A. Salgado, “EPPS16: Nuclear parton distributions with LHC data”, *Eur. Phys. J. C* **77** (2017) 163, arXiv:1612.05741 [hep-ph].
- [2] V. Guzey, E. Kryshen, M. Strikman, and M. Zhalov, “Evidence for nuclear gluon shadowing from the ALICE measurements of PbPb ultraperipheral exclusive J/ψ production”, *Phys. Lett. B* **726** (2013) 290–295, arXiv:1305.1724 [hep-ph].
- [3] V. Guzey, E. Kryshen, M. Strikman, and M. Zhalov, “Nuclear suppression from coherent J/ψ photoproduction at the Large Hadron Collider”, *Phys. Lett. B* **816** (2021) 136202, arXiv:2008.10891 [hep-ph].
- [4] ALICE Collaboration, B. Abelev *et al.*, “Coherent J/ψ photoproduction in ultra-peripheral Pb-Pb collisions at $\sqrt{s_{NN}} = 2.76$ TeV”, *Phys. Lett. B* **718** (2013) 1273–1283, arXiv:1209.3715 [nucl-ex].
- [5] ALICE Collaboration, E. Abbas *et al.*, “Charmonium and e^+e^- pair photoproduction at mid-rapidity in ultra-peripheral Pb-Pb collisions at $\sqrt{s_{NN}}=2.76$ TeV”, *Eur. Phys. J. C* **73** (2013) 2617, arXiv:1305.1467 [nucl-ex].
- [6] CMS Collaboration, V. Khachatryan *et al.*, “Coherent J/ψ photoproduction in ultra-peripheral PbPb collisions at $\sqrt{s_{NN}} = 2.76$ TeV with the CMS experiment”, *Phys. Lett. B* **772** (2017) 489–511, arXiv:1605.06966 [nucl-ex].
- [7] ALICE Collaboration, S. Acharya *et al.*, “Coherent J/ψ photoproduction at forward rapidity in ultra-peripheral Pb-Pb collisions at $\sqrt{s_{NN}} = 5.02$ TeV”, *Phys. Lett. B* **798** (2019) 134926, arXiv:1904.06272 [nucl-ex].
- [8] ALICE Collaboration, S. Acharya *et al.*, “First measurement of the $|t|$ -dependence of coherent J/ψ photonuclear production”, *Phys. Lett. B* **817** (2021) 136280, arXiv:2101.04623 [nucl-ex].
- [9] ALICE Collaboration, S. Acharya *et al.*, “Coherent J/ψ and ψ' photoproduction at midrapidity in ultra-peripheral Pb-Pb collisions at $\sqrt{s_{NN}} = 5.02$ TeV”, *Eur. Phys. J. C* **81** (2021) 712, arXiv:2101.04577 [nucl-ex].
- [10] M. G. Ryskin, “Diffractive J/ψ electroproduction in LLA QCD”, *Z. Phys. C* **57** (1993) 89–92.
- [11] S. R. Klein and H. Mäntysaari, “Imaging the nucleus with high-energy photons”, *Nature Rev. Phys.* **1** (2019) 662–674, arXiv:1910.10858 [hep-ex].
- [12] A. J. Baltz, “The Physics of Ultraperipheral Collisions at the LHC”, *Phys. Rept.* **458** (2008) 1–171, arXiv:0706.3356 [nucl-ex].
- [13] ALICE Collaboration, B. Abelev *et al.*, “Centrality, rapidity and transverse momentum dependence of J/ψ suppression in Pb-Pb collisions at $\sqrt{s_{NN}}=2.76$ TeV”, *Phys. Lett. B* **734** (2014) 314–327, arXiv:1311.0214 [nucl-ex].
- [14] ALICE Collaboration, J. Adam *et al.*, “Differential studies of inclusive J/ψ and $\psi(2S)$ production at forward rapidity in Pb-Pb collisions at $\sqrt{s_{NN}} = 2.76$ TeV”, *JHEP* **05** (2016) 179, arXiv:1506.08804 [nucl-ex].
- [15] ALICE Collaboration, S. Acharya *et al.*, “Studies of J/ψ production at forward rapidity in Pb-Pb collisions at $\sqrt{s_{NN}} = 5.02$ TeV”, *JHEP* **02** (2020) 041, arXiv:1909.03158 [nucl-ex].

- [16] **ALICE** Collaboration, S. Acharya *et al.*, “Centrality and transverse momentum dependence of inclusive J/ψ production at midrapidity in Pb-Pb collisions at $\sqrt{s_{NN}} = 5.02$ TeV”, *Phys. Lett. B* **805** (2020) 135434, arXiv:1910.14404 [nucl-ex].
- [17] T. Matsui and H. Satz, “ J/ψ Suppression by Quark-Gluon Plasma Formation”, *Phys. Lett.* **B178** (1986) 416–422.
- [18] P. Braun-Munzinger and J. Stachel, “(Non)thermal aspects of charmonium production and a new look at J/ψ suppression”, *Phys. Lett.* **B490** (2000) 196–202, arXiv:nucl-th/0007059 [nucl-th].
- [19] R. L. Thews, M. Schroedter, and J. Rafelski, “Enhanced J/ψ production in deconfined quark matter”, *Phys. Rev.* **C63** (2001) 054905, arXiv:hep-ph/0007323 [hep-ph].
- [20] A. Andronic, P. Braun-Munzinger, K. Redlich, and J. Stachel, “Evidence for charmonium generation at the phase boundary in ultra-relativistic nuclear collisions”, *Phys. Lett. B* **652** (2007) 259–261, arXiv:nucl-th/0701079.
- [21] **ALICE** Collaboration, S. Acharya *et al.*, “Inclusive J/ψ production at forward and backward rapidity in p-Pb collisions at $\sqrt{s_{NN}} = 8.16$ TeV”, *JHEP* **07** (2018) 160, arXiv:1805.04381 [nucl-ex].
- [22] **ALICE** Collaboration, S. Acharya *et al.*, “Prompt and non-prompt J/ψ production and nuclear modification at mid-rapidity in p–Pb collisions at $\sqrt{s_{NN}} = 5.02$ TeV”, *Eur. Phys. J. C* **78** (2018) 466, arXiv:1802.00765 [nucl-ex].
- [23] **CMS** Collaboration, A. M. Sirunyan *et al.*, “Measurement of prompt and nonprompt J/ψ production in pp and pPb collisions at $\sqrt{s_{NN}} = 5.02$ TeV”, *Eur. Phys. J. C* **77** (2017) 269, arXiv:1702.01462 [nucl-ex].
- [24] **LHCb** Collaboration, R. Aaij *et al.*, “Prompt and nonprompt J/ψ production and nuclear modification in pPb collisions at $\sqrt{s_{NN}} = 8.16$ TeV”, *Phys. Lett. B* **774** (2017) 159–178, arXiv:1706.07122 [hep-ex].
- [25] **ALICE** Collaboration, J. Adam *et al.*, “Measurement of an excess in the yield of J/ψ at very low p_T in Pb-Pb collisions at $\sqrt{s_{NN}} = 2.76$ TeV”, *Phys. Rev. Lett.* **116** (2016) 222301, arXiv:1509.08802 [nucl-ex].
- [26] W. Shi, W. Zha, and B. Chen, “Charmonium Coherent Photoproduction and Hadroproduction with Effects of Quark Gluon Plasma”, *Phys. Lett. B* **777** (2018) 399–405, arXiv:1710.00332 [nucl-th].
- [27] **STAR** Collaboration, J. Adam *et al.*, “Observation of excess J/ψ yield at very low transverse momenta in Au+Au collisions at $\sqrt{s_{NN}} = 200$ GeV and U+U collisions at $\sqrt{s_{NN}} = 193$ GeV”, *Phys. Rev. Lett.* **123** (2019) 132302, arXiv:1904.11658 [hep-ex].
- [28] **LHCb** Collaboration, R. Aaij *et al.*, “ J/ψ photoproduction in Pb-Pb peripheral collisions at $\sqrt{s_{NN}} = 5$ TeV”, *Phys. Rev. C* **105** (2022) L032201, arXiv:2108.02681 [hep-ex].
- [29] **ATLAS** Collaboration, M. Aaboud *et al.*, “Observation of centrality-dependent acoplanarity for muon pairs produced via two-photon scattering in Pb+Pb collisions at $\sqrt{s_{NN}} = 5.02$ TeV with the ATLAS detector”, *Phys. Rev. Lett.* **121** (2018) 212301, arXiv:1806.08708 [nucl-ex].
- [30] **STAR** Collaboration, J. Adam *et al.*, “Low- p_T e^+e^- pair production in Au+Au collisions at $\sqrt{s_{NN}} = 200$ GeV and U+U collisions at $\sqrt{s_{NN}} = 193$ GeV at STAR”, *Phys. Rev. Lett.* **121** (2018) 132301, arXiv:1806.02295 [hep-ex].

- [31] ALICE Collaboration, S. Acharya *et al.*, “Dielectron production at midrapidity at low transverse momentum in peripheral and semi-peripheral Pb–Pb collisions at $\sqrt{s_{NN}} = 5.02$ TeV”, *JHEP* **06** (2023) 024, arXiv:2204.11732 [nucl-ex].
- [32] M. Gay Ducati and S. Martins, “Heavy meson photoproduction in peripheral AA collisions”, *Phys. Rev. D* **97** (2018) 116013, arXiv:1804.09836 [hep-ph].
- [33] J. Cepila, J. G. Contreras, and M. Krelina, “Coherent and incoherent J/ψ photonuclear production in an energy-dependent hot-spot model”, *Phys. Rev. C* **97** (2018) 024901, arXiv:1711.01855 [hep-ph].
- [34] W. Zha, S. R. Klein, R. Ma, L. Ruan, T. Todoroki, Z. Tang, Z. Xu, C. Yang, Q. Yang, and S. Yang, “Coherent J/ψ photoproduction in hadronic heavy-ion collisions”, *Phys. Rev. C* **97** (2018) 044910, arXiv:1705.01460 [nucl-th].
- [35] M. Klusek-Gawenda and A. Szczurek, “Photoproduction of J/ψ mesons in peripheral and semicentral heavy ion collisions”, *Phys. Rev. C* **93** (2016) 044912, arXiv:1509.03173 [nucl-th].
- [36] L. Jenkovszky, V. Libov, and M. V. T. Machado, “Regge phenomenology and coherent photoproduction of J/ψ in peripheral heavy ion collisions”, *Phys. Lett. B* **827** (2022) 137004, arXiv:2202.02162 [hep-ph].
- [37] J. G. Contreras, “Gluon shadowing at small x from coherent J/ψ photoproduction data at energies available at the CERN Large Hadron Collider”, *Phys. Rev. C* **96** (2017) 015203, arXiv:1610.03350 [nucl-ex].
- [38] ALICE Collaboration, S. Acharya *et al.*, “Inclusive quarkonium production in pp collisions at $\sqrt{s} = 5.02$ TeV”, *Eur. Phys. J. C* **83** (2023) 61, arXiv:2109.15240 [nucl-ex].
- [39] ALICE Collaboration, K. Aamodt *et al.*, “The ALICE experiment at the CERN LHC”, *JINST* **3** (2008) S08002.
- [40] ALICE Collaboration, B. Abelev *et al.*, “Performance of the ALICE Experiment at the CERN LHC”, *Int. J. Mod. Phys. A* **29** (2014) 1430044, arXiv:1402.4476 [nucl-ex].
- [41] ALICE Collaboration, B. Abelev *et al.*, “Centrality determination of Pb–Pb collisions at $\sqrt{s_{NN}} = 2.76$ TeV with ALICE”, *Phys. Rev. C* **88** (2013) 044909, arXiv:1301.4361 [nucl-ex].
- [42] ALICE Collaboration, B. Abelev *et al.*, “Measurement of the Cross Section for Electromagnetic Dissociation with Neutron Emission in Pb–Pb Collisions at $\sqrt{s_{NN}} = 2.76$ TeV”, *Phys. Rev. Lett.* **109** (2012) 252302, arXiv:1203.2436 [nucl-ex].
- [43] ALICE Collaboration, S. Acharya *et al.*, “ALICE luminosity determination for Pb–Pb collisions at $\sqrt{s_{NN}} = 5.02$ TeV”, arXiv:2204.10148 [nucl-ex].
- [44] ALICE Collaboration, J. Adam *et al.*, “Quarkonium signal extraction in ALICE”, ALICE-PUBLIC-2015-006. <https://cds.cern.ch/record/2060096>.
- [45] ALICE Collaboration, S. Acharya *et al.*, “Energy dependence of forward-rapidity J/ψ and $\psi(2S)$ production in pp collisions at the LHC”, *Eur. Phys. J. C* **77** (2017) 392, arXiv:1702.00557 [hep-ex].
- [46] S. R. Klein, J. Nystrand, J. Seger, Y. Gorbunov, and J. Butterworth, “STARlight: A Monte Carlo simulation program for ultra-peripheral collisions of relativistic ions”, *Comput. Phys. Commun.* **212** (2017) 258–268, arXiv:1607.03838 [hep-ph].

- [47] **ALICE** Collaboration, J. Adam *et al.*, “ J/ψ suppression at forward rapidity in Pb-Pb collisions at $\sqrt{s_{NN}} = 5.02$ TeV”, *Phys. Lett. B* **766** (2017) 212–224, arXiv:1606.08197 [nucl-ex].
- [48] **Particle Data Group** Collaboration, P. A. Zyla *et al.*, “Review of Particle Physics”, *PTEP* **2020** (2020) 083C01.
- [49] **ALICE** Collaboration, J. Adam *et al.*, “Centrality dependence of the charged-particle multiplicity density at midrapidity in Pb-Pb collisions at $\sqrt{s_{NN}} = 5.02$ TeV”, *Phys. Rev. Lett.* **116** (2016) 222302, arXiv:1512.06104 [nucl-ex].
- [50] D. d’Enterria and C. Loizides, “Progress in the Glauber Model at Collider Energies”, *Ann. Rev. Nucl. Part. Sci.* **71** (2021) 315–344, arXiv:2011.14909 [hep-ph].
- [51] F. Bossù, Z. C. del Valle, A. de Falco, M. Gagliardi, S. Grigoryan, and G. Martinez Garcia, “Phenomenological interpolation of the inclusive J/ψ cross section to proton-proton collisions at 2.76 TeV and 5.5 TeV”, arXiv:1103.2394 [nucl-ex].
- [52] C. Tsallis, “Possible Generalization of Boltzmann-Gibbs Statistics”, *J. Statist. Phys.* **52** (1988) 479–487.
- [53] **STAR** Collaboration, B. I. Abelev *et al.*, “Strange particle production in p+p collisions at $s^{*(1/2)} = 200$ -GeV”, *Phys. Rev. C* **75** (2007) 064901, arXiv:nucl-ex/0607033.
- [54] X. Zhao and R. Rapp, “Medium Modifications and Production of Charmonia at LHC”, *Nucl. Phys. A* **859** (2011) 114–125, arXiv:1102.2194 [hep-ph].
- [55] Y.-p. Liu, Z. Qu, N. Xu, and P.-f. Zhuang, “ J/ψ Transverse Momentum Distribution in High Energy Nuclear Collisions at RHIC”, *Phys. Lett. B* **678** (2009) 72–76, arXiv:0901.2757 [nucl-th].
- [56] M. Klusek-Gawenda, R. Rapp, W. Schäfer, and A. Szczurek, “Dilepton Radiation in Heavy-Ion Collisions at Small Transverse Momentum”, *Phys. Lett. B* **790** (2019) 339–344, arXiv:1809.07049 [nucl-th].

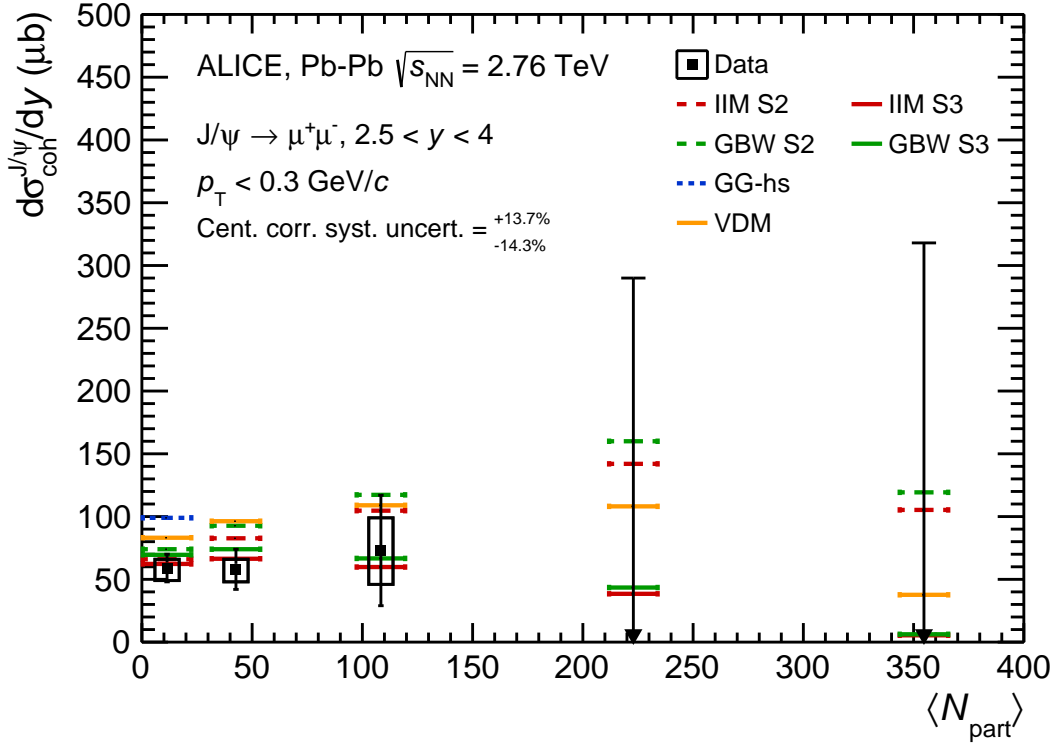


Figure A.1: J/ψ coherent photoproduction cross section as a function of $\langle N_{\text{part}} \rangle$ at forward rapidity in Pb–Pb collisions at $\sqrt{s_{\text{NN}}} = 2.76$ TeV [25]. The vertical bars are the statistical uncertainties and the uncorrelated systematic uncertainties are represented as boxes. The centrality correlated systematic uncertainties are quoted in the legend. Results are compared with theoretical calculations from Ref. [33] (GG-hs), Ref. [32] (IIM S2 and S3, and GBW S2 and S3) and from Ref. [35] with updated Glauber calculations from Ref. [56] (VDM). The figure shows the integral of the cross section measurement as well as the corresponding theoretical model values in each centrality interval. Note that the most central bin, where only an upper limit is given, is half the size of the other intervals. Therefore, to evaluate the centrality dependence of J/ψ coherent photoproduction, both data and theory have to be multiplied by a factor of two.

A J/ψ photoproduction in Pb–Pb collisions at $\sqrt{s_{\text{NN}}} = 2.76$ TeV

Figure A.1 shows the coherent photoproduction measured at $\sqrt{s_{\text{NN}}} = 2.76$ TeV [25]. Empty boxes correspond to the uncorrelated systematic uncertainties. The centrality correlated systematic uncertainty mainly comes from the uncertainties on f_I and f_D , which are asymmetric.





The data are compared with predictions from the same set of models that were described in detail in the paper to which this appendix is associated. The hot-spot model prediction (GG-hs) [33] is only available for the most peripheral centrality interval (70–90%) and it is found to overestimate the data. The other predictions are available for all centrality intervals. The centrality dependence of the models is similar to the one shown at $\sqrt{s_{\text{NN}}} = 5.02$ TeV. The IIM and GBW predictions [32] steadily increase with centrality in the scenario with unmodified photon-nucleus cross section (S2), while the use of an effective cross section where the overlap region between the two nuclei is assumed not to contribute to coherent photoproduction (S3) results in a reduction of the cross section toward more central collisions. However, both scenarios are compatible with data in the current uncertainties. Finally, the VDM calculations are in agreement with data in the most central events while they tend to overestimate data in the 50–70% and 70–90% centrality bins.

B The ALICE Collaboration

S. Acharya ^{123,131}, D. Adamová ⁸⁵, A. Adler⁶⁹, G. Aglieri Rinella ³², M. Agnello ²⁹, N. Agrawal ⁵⁰, Z. Ahammed ¹³¹, S. Ahmad ¹⁵, S.U. Ahn ⁷⁰, I. Ahuja ³⁷, A. Akindinov ¹³⁹, M. Al-Turany ⁹⁷, D. Aleksandrov ¹³⁹, B. Alessandro ⁵⁵, H.M. Alfanda ⁶, R. Alfaro Molina ⁶⁶, B. Ali ¹⁵, Y. Ali¹³, A. Alici ²⁵, N. Alizadehvandchali ¹¹², A. Alkin ³², J. Alme ²⁰, G. Alocco ⁵¹, T. Alt ⁶³, I. Altsybeev ¹³⁹, M.N. Anaam ⁶, C. Andrei ⁴⁵, A. Andronic ¹³⁴, V. Angelov ⁹⁴, F. Antinori ⁵³, P. Antonioli ⁵⁰, C. Anuj ¹⁵, N. Apadula ⁷³, L. Aphecetche ¹⁰², H. Appelshäuser ⁶³, S. Arcelli ²⁵, R. Arnaldi ⁵⁵, I.C. Arsene ¹⁹, M. Arslanok ¹³⁶, A. Augustinus ³², R. Averbeck ⁹⁷, S. Aziz ¹²⁷, M.D. Azmi ¹⁵, A. Badalà ⁵², Y.W. Baek ⁴⁰, X. Bai ⁹⁷, R. Bailhache ⁶³, Y. Bailung ⁴⁷, R. Bala ⁹⁰, A. Balbino ²⁹, A. Baldisseri ¹²⁶, B. Balis ², D. Banerjee ⁴, Z. Banoo ⁹⁰, R. Barbera ²⁶, L. Barioglio ⁹⁵, M. Barlou⁷⁷, G.G. Barnaföldi ¹³⁵, L.S. Barnby ⁸⁴, V. Barret ¹²³, L. Barreto ¹⁰⁸, C. Bartels ¹¹⁵, K. Barth ³², E. Bartsch ⁶³, F. Baruffaldi ²⁷, N. Bastid ¹²³, S. Basu ⁷⁴, G. Batigne ¹⁰², D. Battistini ⁹⁵, B. Batyunya ¹⁴⁰, D. Bauri⁴⁶, J.L. Bazo Alba ¹⁰⁰, I.G. Bearden ⁸², C. Beattie ¹³⁶, P. Becht ⁹⁷, D. Behera ⁴⁷, I. Belikov ¹²⁵, A.D.C. Bell Hechavarria ¹³⁴, F. Bellini ²⁵, R. Bellwied ¹¹², S. Belokurova ¹³⁹, V. Belyaev ¹³⁹, G. Bencedi ^{135,64}, S. Beole ²⁴, A. Bercuci ⁴⁵, Y. Berdnikov ¹³⁹, A. Berdnikova ⁹⁴, L. Bergmann ⁹⁴, M.G. Besoiu ⁶², L. Betev ³², P.P. Bhaduri ¹³¹, A. Bhasin ⁹⁰, I.R. Bhat⁹⁰, M.A. Bhat ⁴, B. Bhattacharjee ⁴¹, L. Bianchi ²⁴, N. Bianchi ⁴⁸, J. Bielčik ³⁵, J. Bielčíková ⁸⁵, J. Biernat ¹⁰⁵, A. Bilandzic ⁹⁵, G. Biro ¹³⁵, S. Biswas ⁴, J.T. Blair ¹⁰⁶, D. Blau ¹³⁹, M.B. Blidaru ⁹⁷, N. Bluhme³⁸, C. Blume ⁶³, G. Boca ^{21,54}, F. Bock ⁸⁶, T. Bodova ²⁰, A. Bogdanov¹³⁹, S. Boi ²², J. Bok ⁵⁷, L. Boldizsár ¹³⁵, A. Bolozdynya ¹³⁹, M. Bombara ³⁷, P.M. Bond ³², G. Bonomi ^{130,54}, H. Borel ¹²⁶, A. Borissov ¹³⁹, H. Bossi ¹³⁶, E. Botta ²⁴, L. Bratrud ⁶³, P. Braun-Munzinger ⁹⁷, M. Bregant ¹⁰⁸, M. Broz ³⁵, G.E. Bruno ^{96,31}, M.D. Buckland ¹¹⁵, D. Budnikov ¹³⁹, H. Buesching ⁶³, S. Bufalino ²⁹, O. Bugnon¹⁰², P. Buhler ¹⁰¹, Z. Buthelezi ^{67,119}, J.B. Butt¹³, A. Bylinkin ¹¹⁴, S.A. Bysiak¹⁰⁵, M. Cai ^{27,6}, H. Caines ¹³⁶, A. Caliva ⁹⁷, E. Calvo Villar ¹⁰⁰, J.M.M. Camacho ¹⁰⁷, P. Camerini ²³, F.D.M. Canedo ¹⁰⁸, M. Carabas ¹²², F. Carnesecchi ³², R. Caron ^{124,126}, J. Castillo Castellanos ¹²⁶, F. Catalano ²⁹, C. Ceballos Sanchez ¹⁴⁰, I. Chakaberia ⁷³, P. Chakraborty ⁴⁶, S. Chandra ¹³¹, S. Chapeland ³², M. Chartier ¹¹⁵, S. Chattopadhyay ¹³¹, S. Chattopadhyay ⁹⁸, T.G. Chavez ⁴⁴, T. Cheng ⁶, C. Cheshkov ¹²⁴, B. Cheynis ¹²⁴, V. Chibante Barroso ³², D.D. Chinellato ¹⁰⁹, E.S. Chizzali ^{11,95}, J. Cho ⁵⁷, S. Cho ⁵⁷, P. Chochula ³², P. Christakoglou ⁸³, C.H. Christensen ⁸², P. Christiansen ⁷⁴, T. Chujo ¹²¹, M. Ciacco ²⁹, C. Cicalo ⁵¹, L. Cifarelli ²⁵, F. Cindolo ⁵⁰, M.R. Ciupek⁹⁷, G. Clai^{III,50}, F. Colamaria ⁴⁹, J.S. Colburn⁹⁹, D. Colella ^{96,31}, A. Collu⁷³, M. Colocci ³², M. Concas ^{IV,55}, G. Conesa Balbastre ⁷², Z. Conesa del Valle ¹²⁷, G. Contin ²³, J.G. Contreras ³⁵, M.L. Coquet ¹²⁶, T.M. Cormier^{I,86}, P. Cortese ^{129,55}, M.R. Cosentino ¹¹⁰, F. Costa ³², S. Costanza ^{21,54}, P. Crochet ¹²³, R. Cruz-Torres ⁷³, E. Cuautle⁶⁴, P. Cui ⁶, L. Cunqueiro⁸⁶, A. Dainese ⁵³, M.C. Danisch ⁹⁴, A. Danu ⁶², P. Das ⁷⁹, P. Das ⁴, S. Das ⁴, S. Dash ⁴⁶, R.M.H. David⁴⁴, A. De Caro ²⁸, G. de Cataldo ⁴⁹, L. De Cilladi ²⁴, J. de Cuveland³⁸, A. De Falco ²², D. De Gruttola ²⁸, N. De Marco ⁵⁵, C. De Martin ²³, S. De Pasquale ²⁸, S. Deb ⁴⁷, H.F. Degenhardt¹⁰⁸, K.R. Deja¹³², R. Del Grande ⁹⁵, L. Dello Stritto ²⁸, W. Deng ⁶, P. Dhankher ¹⁸, D. Di Bari ³¹, A. Di Mauro ³², R.A. Diaz ^{140,7}, T. Dietel ¹¹¹, Y. Ding ^{124,6}, R. Divià ³², D.U. Dixit ¹⁸, Ø. Djuvsland²⁰, U. Dmitrieva ¹³⁹, A. Dobrin ⁶², B. Dönigus ⁶³, A.K. Dubey ¹³¹, J.M. Dubinski ¹³², A. Dubla ⁹⁷, S. Dudi ⁸⁹, P. Dupieux ¹²³, M. Durkac¹⁰⁴, N. Dzalaiova¹², T.M. Eder ¹³⁴, R.J. Ehlers ⁸⁶, V.N. Eikeland²⁰, F. Eisenhut ⁶³, D. Elia ⁴⁹, B. Erazmus ¹⁰², F. Ercolessi ²⁵, F. Erhardt ⁸⁸, M.R. Ersdal²⁰, B. Espagnon ¹²⁷, G. Eulisse ³², D. Evans ⁹⁹, S. Evdokimov ¹³⁹, L. Fabbietti ⁹⁵, M. Faggin ²⁷, J. Faivre ⁷², F. Fan ⁶, W. Fan ⁷³, A. Fantoni ⁴⁸, M. Fasel ⁸⁶, P. Fedichio²⁹, A. Feliciello ⁵⁵, G. Feofilov ¹³⁹, A. Fernández Téllez ⁴⁴, M.B. Ferrer ³², A. Ferrero ¹²⁶, A. Ferretti ²⁴, V.J.G. Feuillard ⁹⁴, J. Figiel ¹⁰⁵, V. Filova ³⁵, D. Finogeev ¹³⁹, F.M. Fionda ⁵¹, G. Fiorenza⁹⁶, F. Flor ¹¹², A.N. Flores ¹⁰⁶, S. Foertsch ⁶⁷, I. Fokin ⁹⁴, S. Fokin ¹³⁹, E. Fragiaco ⁵⁶, E. Frajna ¹³⁵, U. Fuchs ³², N. Funicello ²⁸, C. Furget ⁷², A. Furs ¹³⁹, J.J. Gaardhøje ⁸², M. Gagliardi ²⁴, A.M. Gago ¹⁰⁰, A. Gal¹²⁵, C.D. Galvan ¹⁰⁷, P. Ganoti ⁷⁷, C. Garabatos ⁹⁷, J.R.A. Garcia ⁴⁴, E. Garcia-Solis ⁹, K. Garg ¹⁰², C. Gargiulo ³², A. Garibli⁸⁰, K. Garner¹³⁴, E.F. Gauger ¹⁰⁶, A. Gautam ¹¹⁴, M.B. Gay Ducati ⁶⁵, M. Germain ¹⁰², S.K. Ghosh⁴, M. Giacalone ²⁵, P. Gianotti ⁴⁸, P. Giubellino ^{97,55}, P. Giubilato ²⁷, A.M.C. Glaenger ¹²⁶, P. Glässel ⁹⁴, E. Glimos ¹¹⁸, D.J.Q. Goh⁷⁵, V. Gonzalez ¹³³, L.H. González-Trueba ⁶⁶, S. Gorbunov³⁸, M. Gorgon ², L. Görlich ¹⁰⁵, S. Gotovac³³, V. Grabski ⁶⁶, L.K. Graczykowski ¹³², E. Grecka ⁸⁵, L. Greiner ⁷³, A. Grelli ⁵⁸, C. Grigoras ³², V. Grigoriev ¹³⁹, S. Grigoryan ^{140,1}, F. Grosa ³², J.F. Grosse-Oetringhaus ³², R. Grosso ⁹⁷, D. Grund ³⁵, G.G. Guardiano ¹⁰⁹, R. Guernane ⁷², M. Guilbaud ¹⁰², K. Gulbrandsen ⁸², T. Gunji ¹²⁰, W. Guo ⁶,

A. Gupta ⁹⁰, R. Gupta ⁹⁰, S.P. Guzman ⁴⁴, L. Gyulai ¹³⁵, M.K. Habib ⁹⁷, C. Hadjidakis ¹²⁷, H. Hamagaki ⁷⁵, M. Hamid ⁶, Y. Han ¹³⁷, R. Hannigan ¹⁰⁶, M.R. Haque ¹³², A. Harlanderova ⁹⁷, J.W. Harris ¹³⁶, A. Harton ⁹, J.A. Hasenbichler ³², H. Hassan ⁸⁶, D. Hatzifotiadou ⁵⁰, P. Hauer ⁴², L.B. Havener ¹³⁶, S.T. Heckel ⁹⁵, E. Hellbär ⁹⁷, H. Helstrup ³⁴, T. Herman ³⁵, G. Herrera Corral ⁸, F. Herrmann ¹³⁴, K.F. Hetland ³⁴, B. Heybeck ⁶³, H. Hillemanns ³², C. Hills ¹¹⁵, B. Hippolyte ¹²⁵, B. Hofman ⁵⁸, B. Hohlweger ⁸³, J. Honermann ¹³⁴, G.H. Hong ¹³⁷, D. Horak ³⁵, A. Horzyk ², R. Hosokawa ¹⁴, Y. Hou ⁶, P. Hristov ³², C. Hughes ¹¹⁸, P. Huhn ⁶³, L.M. Huhta ¹¹³, C.V. Hulse ¹²⁷, T.J. Humanic ⁸⁷, H. Hushnud ⁹⁸, A. Hutson ¹¹², D. Hutter ³⁸, J.P. Iddon ¹¹⁵, R. Ilkaev ¹³⁹, H. Ilyas ¹³, M. Inaba ¹²¹, G.M. Innocenti ³², M. Ippolitov ¹³⁹, A. Isakov ⁸⁵, T. Isidori ¹¹⁴, M.S. Islam ⁹⁸, M. Ivanov ⁹⁷, V. Ivanov ¹³⁹, V. Izucheev ¹³⁹, M. Jablonski ², B. Jacak ⁷³, N. Jacazio ³², P.M. Jacobs ⁷³, S. Jadlovská ¹⁰⁴, J. Jadlovsky ¹⁰⁴, L. Jaffe ³⁸, C. Jahnke ¹⁰⁹, M.A. Janik ¹³², T. Janson ⁶⁹, M. Jercic ⁸⁸, O. Jevons ⁹⁹, A.A.P. Jimenez ⁶⁴, F. Jonas ⁸⁶, P.G. Jones ⁹⁹, J.M. Jowett ^{32,97}, J. Jung ⁶³, M. Jung ⁶³, A. Junique ³², A. Jusko ⁹⁹, M.J. Kabus ^{32,132}, J. Kaewjai ¹⁰³, P. Kalinak ⁵⁹, A.S. Kalteyer ⁹⁷, A. Kalweit ³², V. Kaplin ¹³⁹, A. Karasu Uysal ⁷¹, D. Karatovic ⁸⁸, O. Karavichev ¹³⁹, T. Karavicheva ¹³⁹, P. Karczmarczyk ¹³², E. Karpechev ¹³⁹, V. Kashyap ⁷⁹, A. Kazantsev ¹³⁹, U. Keschull ⁶⁹, R. Keidel ¹³⁸, D.L.D. Keijdener ⁵⁸, M. Keil ³², B. Ketzer ⁴², A.M. Khan ⁶, S. Khan ¹⁵, A. Khanzadeev ¹³⁹, Y. Kharlov ¹³⁹, A. Khatun ¹⁵, A. Khuntia ¹⁰⁵, B. Kileng ³⁴, B. Kim ¹⁶, C. Kim ¹⁶, D.J. Kim ¹¹³, E.J. Kim ⁶⁸, J. Kim ¹³⁷, J.S. Kim ⁴⁰, J. Kim ⁹⁴, J. Kim ⁶⁸, M. Kim ⁹⁴, S. Kim ¹⁷, T. Kim ¹³⁷, S. Kirsch ⁶³, I. Kisel ³⁸, S. Kiselev ¹³⁹, A. Kisiel ¹³², J.P. Kitowski ², J.L. Klay ⁵, J. Klein ³², S. Klein ⁷³, C. Klein-Bösing ¹³⁴, M. Kleiner ⁶³, T. Klemenz ⁹⁵, A. Kluge ³², A.G. Knospe ¹¹², C. Kobdaj ¹⁰³, T. Kollegger ⁹⁷, A. Kondratyev ¹⁴⁰, N. Kondratyeva ¹³⁹, E. Kondratyuk ¹³⁹, J. Konig ⁶³, S.A. Konigstorfer ⁹⁵, P.J. Konopka ³², G. Kornakov ¹³², S.D. Koryciak ², A. Kotliarov ⁸⁵, O. Kovalenko ⁷⁸, V. Kovalenko ¹³⁹, M. Kowalski ¹⁰⁵, I. Králík ⁵⁹, A. Kravčáková ³⁷, L. Kreis ⁹⁷, M. Krivda ^{99,59}, F. Krizek ⁸⁵, K. Krizkova Gajdosova ³⁵, M. Kroesen ⁹⁴, M. Krüger ⁶³, D.M. Krupova ³⁵, E. Kryshen ¹³⁹, M. Krzewicki ³⁸, V. Kučera ³², C. Kuhn ¹²⁵, P.G. Kuijter ⁸³, T. Kumaoka ¹²¹, D. Kumar ¹³¹, L. Kumar ⁸⁹, N. Kumar ⁸⁹, S. Kundu ³², P. Kurashvili ⁷⁸, A. Kurepin ¹³⁹, A.B. Kurepin ¹³⁹, S. Kushpil ⁸⁵, J. Kvapil ⁹⁹, M.J. Kwon ⁵⁷, J.Y. Kwon ⁵⁷, Y. Kwon ¹³⁷, S.L. La Pointe ³⁸, P. La Rocca ²⁶, Y.S. Lai ⁷³, A. Lakrathok ¹⁰³, M. Lamanna ³², R. Langoy ¹¹⁷, P. Larionov ⁴⁸, E. Laudi ³², L. Lautner ^{32,95}, R. Lavicka ¹⁰¹, T. Lazareva ¹³⁹, R. Lea ^{130,54}, J. Lehrbach ³⁸, R.C. Lemmon ⁸⁴, I. León Monzón ¹⁰⁷, M.M. Lesch ⁹⁵, E.D. Lesser ¹⁸, M. Lettrich ⁹⁵, P. Lévai ¹³⁵, X. Li ¹⁰, X.L. Li ⁶, J. Lien ¹¹⁷, R. Lietava ⁹⁹, B. Lim ¹⁶, S.H. Lim ¹⁶, V. Lindenstruth ³⁸, A. Lindner ⁴⁵, C. Lippmann ⁹⁷, A. Liu ¹⁸, D.H. Liu ⁶, J. Liu ¹¹⁵, I.M. Lofnes ²⁰, V. Loginov ¹³⁹, C. Loizides ⁸⁶, P. Loncar ³³, J.A. Lopez ⁹⁴, X. Lopez ¹²³, E. López Torres ⁷, P. Lu ^{97,116}, J.R. Luhder ¹³⁴, M. Lunardon ²⁷, G. Luparello ⁵⁶, Y.G. Ma ³⁹, A. Maevskaya ¹³⁹, M. Mager ³², T. Mahmoud ⁴², A. Maire ¹²⁵, M. Malaev ¹³⁹, N.M. Malik ⁹⁰, Q.W. Malik ¹⁹, S.K. Malik ⁹⁰, L. Malinina ^{VII,140}, D. Mal'Kevich ¹³⁹, D. Mallick ⁷⁹, N. Mallick ⁴⁷, G. Mandaglio ^{30,52}, V. Manko ¹³⁹, F. Manso ¹²³, V. Manzari ⁴⁹, Y. Mao ⁶, G.V. Margagliotti ²³, A. Margotti ⁵⁰, A. Marín ⁹⁷, C. Markert ¹⁰⁶, M. Marquard ⁶³, N.A. Martin ⁹⁴, P. Martinengo ³², J.L. Martinez ¹¹², M.I. Martínez ⁴⁴, G. Martínez García ¹⁰², S. Masciocchi ⁹⁷, M. Masera ²⁴, A. Masoni ⁵¹, L. Massacrier ¹²⁷, A. Mastroserio ^{128,49}, A.M. Mathis ⁹⁵, O. Matonoha ⁷⁴, P.F.T. Matuoka ¹⁰⁸, A. Matyja ¹⁰⁵, C. Mayer ¹⁰⁵, A.L. Mazuecos ³², F. Mazzaschi ²⁴, M. Mazzilli ³², J.E. Mdhuli ¹¹⁹, A.F. Mechler ⁶³, Y. Melikyan ¹³⁹, A. Menchaca-Rocha ⁶⁶, E. Meninno ^{101,28}, A.S. Menon ¹¹², M. Meres ¹², S. Mhlanga ^{111,67}, Y. Miake ¹²¹, L. Micheletti ⁵⁵, L.C. Migliorin ¹²⁴, D.L. Mihaylov ⁹⁵, K. Mikhaylov ^{140,139}, A.N. Mishra ¹³⁵, D. Miśkowiec ⁹⁷, A. Modak ⁴, A.P. Mohanty ⁵⁸, B. Mohanty ⁷⁹, M. Mohisin Khan ^{V,15}, M.A. Molander ⁴³, Z. Moravcova ⁸², C. Mordasini ⁹⁵, D.A. Moreira De Godoy ¹³⁴, I. Morozov ¹³⁹, A. Morsch ³², T. Mrnjavac ³², V. Muccifora ⁴⁸, E. Mudnic ³³, S. Muhuri ¹³¹, J.D. Mulligan ⁷³, A. Mulliri ²², M.G. Munhoz ¹⁰⁸, R.H. Munzer ⁶³, H. Murakami ¹²⁰, S. Murray ¹¹¹, L. Musa ³², J. Musinsky ⁵⁹, J.W. Myrcha ¹³², B. Naik ¹¹⁹, R. Nair ⁷⁸, B.K. Nandi ⁴⁶, R. Nania ⁵⁰, E. Nappi ⁴⁹, A.F. Nassirpour ⁷⁴, A. Nath ⁹⁴, C. Nattrass ¹¹⁸, A. Neagu ¹⁹, A. Negru ¹²², L. Nellen ⁶⁴, S.V. Nesbo ³⁴, G. Neskovic ³⁸, D. Nesterov ¹³⁹, B.S. Nielsen ⁸², E.G. Nielsen ⁸², S. Nikolaev ¹³⁹, S. Nikulin ¹³⁹, V. Nikulin ¹³⁹, F. Noferini ⁵⁰, S. Noh ¹¹, P. Nomokonov ¹⁴⁰, J. Norman ¹¹⁵, N. Novitzky ¹²¹, P. Nowakowski ¹³², A. Nyanin ¹³⁹, J. Nystrand ²⁰, M. Ogino ⁷⁵, A. Ohlson ⁷⁴, V.A. Okorokov ¹³⁹, J. Olińczak ¹³², A.C. Oliveira Da Silva ¹¹⁸, M.H. Oliver ¹³⁶, A. Onnerstad ¹¹³, C. Oppedisano ⁵⁵, A. Ortiz Velasquez ⁶⁴, A. Oskarsson ⁷⁴, J. Otwinowski ¹⁰⁵, M. Oya ⁹², K. Oyama ⁷⁵, Y. Pachmayer ⁹⁴, S. Padhan ⁴⁶, D. Pagano ^{130,54}, G. Paic ⁶⁴, A. Palasciano ⁴⁹, S. Panebianco ¹²⁶, J. Park ⁵⁷, J.E. Parkkila ^{32,113}, S.P. Pathak ¹¹², R.N. Patra ⁹⁰, B. Paul ²², H. Pei ⁶, T. Peitzmann ⁵⁸, X. Peng ⁶,

L.G. Pereira⁶⁵, H. Pereira Da Costa¹²⁶, D. Peresunko¹³⁹, G.M. Perez⁷, S. Perrin¹²⁶, Y. Pestov¹³⁹,
 V. Petráček³⁵, V. Petrov¹³⁹, M. Petrovici⁴⁵, R.P. Pezzi^{102,65}, S. Piano⁵⁶, M. Pikna¹², P. Pillot¹⁰²,
 O. Pinazza^{50,32}, L. Pinsky¹¹², C. Pinto^{95,26}, S. Pisano⁴⁸, M. Płoskoń⁷³, M. Planinic⁸⁸, F. Pliquet⁶³,
 M.G. Poghosyan⁸⁶, S. Politano²⁹, N. Poljak⁸⁸, A. Pop⁴⁵, S. Porteboeuf-Houssais¹²³, J. Porter⁷³,
 V. Pozdniakov¹⁴⁰, S.K. Prasad⁴, S. Prasad⁴⁷, R. Preghenella⁵⁰, F. Prino⁵⁵, C.A. Pruneau¹³³,
 I. Pshenichnov¹³⁹, M. Puccio³², S. Qiu⁸³, L. Quaglia²⁴, R.E. Quishpe¹¹², S. Ragoni⁹⁹,
 A. Rakotozafindrabe¹²⁶, L. Ramello^{129,55}, F. Rami¹²⁵, S.A.R. Ramirez⁴⁴, T.A. Rancien⁷²,
 R. Raniwala⁹¹, S. Raniwala⁹¹, S.S. Räsänen⁴³, R. Rath⁴⁷, I. Ravasenga⁸³, K.F. Read^{86,118},
 A.R. Redelbach³⁸, K. Redlich^{VI,78}, A. Rehman²⁰, P. Reichelt⁶³, F. Reidt³², H.A. Reme-Ness³⁴,
 Z. Rescakova³⁷, K. Reyers⁹⁴, A. Riabov¹³⁹, V. Riabov¹³⁹, R. Ricci²⁸, T. Richert⁷⁴, M. Richter¹⁹,
 W. Riegler³², F. Riggi²⁶, C. Ristea⁶², M. Rodríguez Cahuantzi⁴⁴, K. Røed¹⁹, R. Rogalev¹³⁹,
 E. Rogochaya¹⁴⁰, T.S. Rogoschinski⁶³, D. Rohr³², D. Röhrich²⁰, P.F. Rojas⁴⁴, S. Rojas Torres³⁵,
 P.S. Rokita¹³², F. Ronchetti⁴⁸, A. Rosano^{30,52}, E.D. Rosas⁶⁴, A. Rossi⁵³, A. Roy⁴⁷, P. Roy⁹⁸,
 S. Roy⁴⁶, N. Rubini²⁵, D. Ruggiano¹³², R. Rui²³, B. Rumyantsev¹⁴⁰, P.G. Russek², R. Russo⁸³,
 A. Rustamov⁸⁰, E. Ryabinkin¹³⁹, Y. Ryabov¹³⁹, A. Rybicki¹⁰⁵, H. Rytkonen¹¹³, W. Rzesa¹³²,
 O.A.M. Saarimaki⁴³, R. Sadek¹⁰², S. Sadovsky¹³⁹, J. Saetre²⁰, K. Šafařík³⁵, S.K. Saha¹³¹,
 S. Saha⁷⁹, B. Sahoo⁴⁶, P. Sahoo⁴⁶, R. Sahoo⁴⁷, S. Sahoo⁶⁰, D. Sahu⁴⁷, P.K. Sahu⁶⁰, J. Saini¹³¹,
 K. Sajdakova³⁷, S. Sakai¹²¹, M.P. Salvan⁹⁷, S. Sambyal⁹⁰, T.B. Saramela¹⁰⁸, D. Sarkar¹³³, N. Sarkar¹³¹,
 P. Sarma⁴¹, V. Sarritzu²², V.M. Sarti⁹⁵, M.H.P. Sas¹³⁶, J. Schambach⁸⁶, H.S. Scheid⁶³,
 C. Schiaua⁴⁵, R. Schicker⁹⁴, A. Schmah⁹⁴, C. Schmidt⁹⁷, H.R. Schmidt⁹³, M.O. Schmidt³²,
 M. Schmidt⁹³, N.V. Schmidt^{86,63}, A.R. Schmier¹¹⁸, R. Schotter¹²⁵, J. Schukraft³², K. Schwarz⁹⁷,
 K. Schweda⁹⁷, G. Scioli²⁵, E. Scomarini⁵⁵, J.E. Seger¹⁴, Y. Sekiguchi¹²⁰, D. Sekihata¹²⁰,
 I. Selyuzhenkov^{97,139}, S. Senyukov¹²⁵, J.J. Seo⁵⁷, D. Serebryakov¹³⁹, L. Šerkšnytė⁹⁵,
 A. Sevcenco⁶², T.J. Shaba⁶⁷, A. Shabanov¹³⁹, A. Shabetai¹⁰², R. Shahoyan³², W. Shaikh⁹⁸,
 A. Shangaraev¹³⁹, A. Sharma⁸⁹, D. Sharma⁴⁶, H. Sharma¹⁰⁵, M. Sharma⁹⁰, N. Sharma⁸⁹,
 S. Sharma⁹⁰, U. Sharma⁹⁰, A. Shatat¹²⁷, O. Sheibani¹¹², K. Shigaki⁹², M. Shimomura⁷⁶,
 S. Shirinkin¹³⁹, Q. Shou³⁹, Y. Sibiriak¹³⁹, S. Siddhanta⁵¹, T. Siemiarz⁷⁸, T.F. Silva¹⁰⁸,
 D. Silvermyr⁷⁴, T. Simantathammakul¹⁰³, R. Simeonov³⁶, G. Simonetti³², B. Singh⁹⁰, B. Singh⁹⁵,
 R. Singh⁷⁹, R. Singh⁹⁰, R. Singh⁴⁷, V.K. Singh¹³¹, V. Singhal¹³¹, T. Sinha⁹⁸, B. Sitar¹²,
 M. Sitta^{129,55}, T.B. Skaali¹⁹, G. Skorodumovs⁹⁴, M. Slupecki⁴³, N. Smirnov¹³⁶, R.J.M. Snellings⁵⁸,
 E.H. Solheim¹⁹, C. Soncco¹⁰⁰, J. Song¹¹², A. Songmoolnak¹⁰³, F. Soramel²⁷, S.P. Sorensen¹¹⁸, R. Soto
 Camacho⁴⁴, R. Spijkers⁸³, I. Sputowska¹⁰⁵, J. Staa⁷⁴, J. Stachel⁹⁴, I. Stan⁶², P.J. Steffanic¹¹⁸,
 S.F. Stiefelmaier⁹⁴, D. Stocco¹⁰², I. Storehaug¹⁹, M.M. Stoksett³⁴, P. Stratmann¹³⁴, S. Strazzi²⁵,
 C.P. Stylianidis⁸³, A.A.P. Suaide¹⁰⁸, C. Suire¹²⁷, M. Sukhanov¹³⁹, M. Suljic³², V. Sumberia⁹⁰,
 S. Sumowidagdo⁸¹, S. Swain⁶⁰, A. Szabo¹², I. Szarka¹², U. Tabassam¹³, S.F. Taghavi⁹⁵,
 G. Taillepied^{97,123}, J. Takahashi¹⁰⁹, G.J. Tambave²⁰, S. Tang^{123,6}, Z. Tang¹¹⁶, J.D. Tapia Takaki¹¹⁴,
 N. Tapus¹²², L.A. Tarasovicova¹³⁴, M. Tarhini¹⁰², M.G. Tarzila⁴⁵, A. Tauro³², A. Telesca³²,
 L. Terlizzi²⁴, C. Terrevoli¹¹², G. Tersimonov³, S. Thakur¹³¹, D. Thomas¹⁰⁶, R. Tieulent¹²⁴,
 A. Tikhonov¹³⁹, A.R. Timmins¹¹², M. Tkacik¹⁰⁴, T. Tkacik¹⁰⁴, A. Toia⁶³, N. Topilskaya¹³⁹,
 M. Toppi⁴⁸, F. Torres-Acosta¹⁸, T. Tork¹²⁷, A.G. Torres Ramos³¹, A. Trifiro^{30,52}, A.S. Triolo^{30,52},
 S. Tripathy⁵⁰, T. Tripathy⁴⁶, S. Trogolo³², V. Trubnikov³, W.H. Trzaska¹¹³, T.P. Trzcinski¹³²,
 R. Turrisi⁵³, T.S. Tveter¹⁹, K. Ullaland²⁰, B. Ulukutlu⁹⁵, A. Uras¹²⁴, M. Urioni^{54,130},
 G.L. Usai²², M. Vala³⁷, N. Valle²¹, S. Vallero⁵⁵, L.V.R. van Doremalen⁵⁸, M. van Leeuwen⁸³, C.A. van
 Veen⁹⁴, R.J.G. van Weelden⁸³, P. Vande Vyvre³², D. Varga¹³⁵, Z. Varga¹³⁵, M. Varga-Kofarago¹³⁵,
 M. Vasileiou⁷⁷, A. Vasiliev¹³⁹, O. Vázquez Doce⁹⁵, O. Vazquez Rueda⁷⁴, V. Vechernin¹³⁹,
 E. Vercellin²⁴, S. Vergara Limón⁴⁴, L. Vermunt⁵⁸, R. Vértesi¹³⁵, M. Verweij⁵⁸, L. Vickovic³³,
 Z. Vilakazi¹¹⁹, O. Villalobos Baillie⁹⁹, G. Vino⁴⁹, A. Vinogradov¹³⁹, T. Virgili²⁸, V. Vislavicius⁸²,
 A. Vodopyanov¹⁴⁰, B. Volkel³², M.A. Völkl⁹⁴, K. Voloshin¹³⁹, S.A. Voloshin¹³³, G. Volpe³¹, B. von
 Haller³², I. Vorobyev⁹⁵, N. Vozniuk¹³⁹, J. Vrláková³⁷, B. Wagner²⁰, C. Wang³⁹, D. Wang³⁹,
 M. Weber¹⁰¹, A. Wegrzynek³², F.T. Weiglhofer³⁸, S.C. Wenzel³², J.P. Wessels¹³⁴,
 S.L. Weyhmiller¹³⁶, J. Wiechula⁶³, J. Wikne¹⁹, G. Wilk⁷⁸, J. Wilkinson⁹⁷, G.A. Willems¹³⁴,
 B. Windelband⁹⁴, M. Winn¹²⁶, J.R. Wright¹⁰⁶, W. Wu³⁹, Y. Wu¹¹⁶, R. Xu⁶, A.K. Yadav¹³¹,
 S. Yalcin⁷¹, Y. Yamaguchi⁹², K. Yamakawa⁹², S. Yang²⁰, S. Yano⁹², Z. Yin⁶, I.-K. Yoo¹⁶,
 J.H. Yoon⁵⁷, S. Yuan²⁰, A. Yuncu⁹⁴, V. Zaccolo²³, C. Zampolli³², H.J.C. Zanoli⁵⁸, F. Zanone⁹⁴,
 N. Zardoshti^{32,99}, A. Zarochentsev¹³⁹, P. Závada⁶¹, N. Zaviyalov¹³⁹, M. Zhalov¹³⁹, B. Zhang⁶,
 S. Zhang³⁹, X. Zhang⁶, Y. Zhang¹¹⁶, M. Zhao¹⁰, V. ZhЕРЕbchevskii¹³⁹, Y. Zhi¹⁰, N. Zhigareva¹³⁹,

D. Zhou ⁶, Y. Zhou ⁸², J. Zhu ^{97,6}, Y. Zhu⁶, G. Zinovjev^{1,3}, N. Zurlo ^{130,54}

Affiliation Notes

^I Deceased

^{II} Also at: Max-Planck-Institut für Physik, Munich, Germany

^{III} Also at: Italian National Agency for New Technologies, Energy and Sustainable Economic Development (ENEA), Bologna, Italy

^{IV} Also at: Dipartimento DET del Politecnico di Torino, Turin, Italy

^V Also at: Department of Applied Physics, Aligarh Muslim University, Aligarh, India

^{VI} Also at: Institute of Theoretical Physics, University of Wrocław, Poland

^{VII} Also at: An institution covered by a cooperation agreement with CERN

Collaboration Institutes

¹ A.I. Alikhanyan National Science Laboratory (Yerevan Physics Institute) Foundation, Yerevan, Armenia

² AGH University of Krakow, Cracow, Poland

³ Bogolyubov Institute for Theoretical Physics, National Academy of Sciences of Ukraine, Kiev, Ukraine

⁴ Bose Institute, Department of Physics and Centre for Astroparticle Physics and Space Science (CAPSS), Kolkata, India

⁵ California Polytechnic State University, San Luis Obispo, California, United States

⁶ Central China Normal University, Wuhan, China

⁷ Centro de Aplicaciones Tecnológicas y Desarrollo Nuclear (CEADEN), Havana, Cuba

⁸ Centro de Investigación y de Estudios Avanzados (CINVESTAV), Mexico City and Mérida, Mexico

⁹ Chicago State University, Chicago, Illinois, United States

¹⁰ China Institute of Atomic Energy, Beijing, China

¹¹ Chungbuk National University, Cheongju, Republic of Korea

¹² Comenius University Bratislava, Faculty of Mathematics, Physics and Informatics, Bratislava, Slovak Republic

¹³ COMSATS University Islamabad, Islamabad, Pakistan

¹⁴ Creighton University, Omaha, Nebraska, United States

¹⁵ Department of Physics, Aligarh Muslim University, Aligarh, India

¹⁶ Department of Physics, Pusan National University, Pusan, Republic of Korea

¹⁷ Department of Physics, Sejong University, Seoul, Republic of Korea

¹⁸ Department of Physics, University of California, Berkeley, California, United States

¹⁹ Department of Physics, University of Oslo, Oslo, Norway

²⁰ Department of Physics and Technology, University of Bergen, Bergen, Norway

²¹ Dipartimento di Fisica, Università di Pavia, Pavia, Italy

²² Dipartimento di Fisica dell'Università and Sezione INFN, Cagliari, Italy

²³ Dipartimento di Fisica dell'Università and Sezione INFN, Trieste, Italy

²⁴ Dipartimento di Fisica dell'Università and Sezione INFN, Turin, Italy

²⁵ Dipartimento di Fisica e Astronomia dell'Università and Sezione INFN, Bologna, Italy

²⁶ Dipartimento di Fisica e Astronomia dell'Università and Sezione INFN, Catania, Italy

²⁷ Dipartimento di Fisica e Astronomia dell'Università and Sezione INFN, Padova, Italy

²⁸ Dipartimento di Fisica 'E.R. Caianiello' dell'Università and Gruppo Collegato INFN, Salerno, Italy

²⁹ Dipartimento DISAT del Politecnico and Sezione INFN, Turin, Italy

³⁰ Dipartimento di Scienze MIFT, Università di Messina, Messina, Italy

³¹ Dipartimento Interateneo di Fisica 'M. Merlin' and Sezione INFN, Bari, Italy

³² European Organization for Nuclear Research (CERN), Geneva, Switzerland

³³ Faculty of Electrical Engineering, Mechanical Engineering and Naval Architecture, University of Split, Split, Croatia

³⁴ Faculty of Engineering and Science, Western Norway University of Applied Sciences, Bergen, Norway

³⁵ Faculty of Nuclear Sciences and Physical Engineering, Czech Technical University in Prague, Prague, Czech Republic

³⁶ Faculty of Physics, Sofia University, Sofia, Bulgaria

³⁷ Faculty of Science, P.J. Šafárik University, Košice, Slovak Republic

³⁸ Frankfurt Institute for Advanced Studies, Johann Wolfgang Goethe-Universität Frankfurt, Frankfurt, Germany

- ³⁹ Fudan University, Shanghai, China
⁴⁰ Gangneung-Wonju National University, Gangneung, Republic of Korea
⁴¹ Gauhati University, Department of Physics, Guwahati, India
⁴² Helmholtz-Institut für Strahlen- und Kernphysik, Rheinische Friedrich-Wilhelms-Universität Bonn, Bonn, Germany
⁴³ Helsinki Institute of Physics (HIP), Helsinki, Finland
⁴⁴ High Energy Physics Group, Universidad Autónoma de Puebla, Puebla, Mexico
⁴⁵ Horia Hulubei National Institute of Physics and Nuclear Engineering, Bucharest, Romania
⁴⁶ Indian Institute of Technology Bombay (IIT), Mumbai, India
⁴⁷ Indian Institute of Technology Indore, Indore, India
⁴⁸ INFN, Laboratori Nazionali di Frascati, Frascati, Italy
⁴⁹ INFN, Sezione di Bari, Bari, Italy
⁵⁰ INFN, Sezione di Bologna, Bologna, Italy
⁵¹ INFN, Sezione di Cagliari, Cagliari, Italy
⁵² INFN, Sezione di Catania, Catania, Italy
⁵³ INFN, Sezione di Padova, Padova, Italy
⁵⁴ INFN, Sezione di Pavia, Pavia, Italy
⁵⁵ INFN, Sezione di Torino, Turin, Italy
⁵⁶ INFN, Sezione di Trieste, Trieste, Italy
⁵⁷ Inha University, Incheon, Republic of Korea
⁵⁸ Institute for Gravitational and Subatomic Physics (GRASP), Utrecht University/Nikhef, Utrecht, Netherlands
⁵⁹ Institute of Experimental Physics, Slovak Academy of Sciences, Košice, Slovak Republic
⁶⁰ Institute of Physics, Homi Bhabha National Institute, Bhubaneswar, India
⁶¹ Institute of Physics of the Czech Academy of Sciences, Prague, Czech Republic
⁶² Institute of Space Science (ISS), Bucharest, Romania
⁶³ Institut für Kernphysik, Johann Wolfgang Goethe-Universität Frankfurt, Frankfurt, Germany
⁶⁴ Instituto de Ciencias Nucleares, Universidad Nacional Autónoma de México, Mexico City, Mexico
⁶⁵ Instituto de Física, Universidade Federal do Rio Grande do Sul (UFRGS), Porto Alegre, Brazil
⁶⁶ Instituto de Física, Universidad Nacional Autónoma de México, Mexico City, Mexico
⁶⁷ iThemba LABS, National Research Foundation, Somerset West, South Africa
⁶⁸ Jeonbuk National University, Jeonju, Republic of Korea
⁶⁹ Johann-Wolfgang-Goethe Universität Frankfurt Institut für Informatik, Fachbereich Informatik und Mathematik, Frankfurt, Germany
⁷⁰ Korea Institute of Science and Technology Information, Daejeon, Republic of Korea
⁷¹ KTO Karatay University, Konya, Turkey
⁷² Laboratoire de Physique Subatomique et de Cosmologie, Université Grenoble-Alpes, CNRS-IN2P3, Grenoble, France
⁷³ Lawrence Berkeley National Laboratory, Berkeley, California, United States
⁷⁴ Lund University Department of Physics, Division of Particle Physics, Lund, Sweden
⁷⁵ Nagasaki Institute of Applied Science, Nagasaki, Japan
⁷⁶ Nara Women's University (NWU), Nara, Japan
⁷⁷ National and Kapodistrian University of Athens, School of Science, Department of Physics, Athens, Greece
⁷⁸ National Centre for Nuclear Research, Warsaw, Poland
⁷⁹ National Institute of Science Education and Research, Homi Bhabha National Institute, Jatni, India
⁸⁰ National Nuclear Research Center, Baku, Azerbaijan
⁸¹ National Research and Innovation Agency - BRIN, Jakarta, Indonesia
⁸² Niels Bohr Institute, University of Copenhagen, Copenhagen, Denmark
⁸³ Nikhef, National institute for subatomic physics, Amsterdam, Netherlands
⁸⁴ Nuclear Physics Group, STFC Daresbury Laboratory, Daresbury, United Kingdom
⁸⁵ Nuclear Physics Institute of the Czech Academy of Sciences, Husinec-Řež, Czech Republic
⁸⁶ Oak Ridge National Laboratory, Oak Ridge, Tennessee, United States
⁸⁷ Ohio State University, Columbus, Ohio, United States
⁸⁸ Physics department, Faculty of science, University of Zagreb, Zagreb, Croatia
⁸⁹ Physics Department, Panjab University, Chandigarh, India
⁹⁰ Physics Department, University of Jammu, Jammu, India
⁹¹ Physics Department, University of Rajasthan, Jaipur, India

- ⁹² Physics Program and International Institute for Sustainability with Knotted Chiral Meta Matter (SKCM2), Hiroshima University, Hiroshima, Japan
- ⁹³ Physikalisches Institut, Eberhard-Karls-Universität Tübingen, Tübingen, Germany
- ⁹⁴ Physikalisches Institut, Ruprecht-Karls-Universität Heidelberg, Heidelberg, Germany
- ⁹⁵ Physik Department, Technische Universität München, Munich, Germany
- ⁹⁶ Politecnico di Bari and Sezione INFN, Bari, Italy
- ⁹⁷ Research Division and ExtreMe Matter Institute EMMI, GSI Helmholtzzentrum für Schwerionenforschung GmbH, Darmstadt, Germany
- ⁹⁸ Saha Institute of Nuclear Physics, Homi Bhabha National Institute, Kolkata, India
- ⁹⁹ School of Physics and Astronomy, University of Birmingham, Birmingham, United Kingdom
- ¹⁰⁰ Sección Física, Departamento de Ciencias, Pontificia Universidad Católica del Perú, Lima, Peru
- ¹⁰¹ Stefan Meyer Institut für Subatomare Physik (SMI), Vienna, Austria
- ¹⁰² SUBATECH, IMT Atlantique, Nantes Université, CNRS-IN2P3, Nantes, France
- ¹⁰³ Suranaree University of Technology, Nakhon Ratchasima, Thailand
- ¹⁰⁴ Technical University of Košice, Košice, Slovak Republic
- ¹⁰⁵ The Henryk Niewodniczanski Institute of Nuclear Physics, Polish Academy of Sciences, Cracow, Poland
- ¹⁰⁶ The University of Texas at Austin, Austin, Texas, United States
- ¹⁰⁷ Universidad Autónoma de Sinaloa, Culiacán, Mexico
- ¹⁰⁸ Universidade de São Paulo (USP), São Paulo, Brazil
- ¹⁰⁹ Universidade Estadual de Campinas (UNICAMP), Campinas, Brazil
- ¹¹⁰ Universidade Federal do ABC, Santo Andre, Brazil
- ¹¹¹ University of Cape Town, Cape Town, South Africa
- ¹¹² University of Houston, Houston, Texas, United States
- ¹¹³ University of Jyväskylä, Jyväskylä, Finland
- ¹¹⁴ University of Kansas, Lawrence, Kansas, United States
- ¹¹⁵ University of Liverpool, Liverpool, United Kingdom
- ¹¹⁶ University of Science and Technology of China, Hefei, China
- ¹¹⁷ University of South-Eastern Norway, Kongsberg, Norway
- ¹¹⁸ University of Tennessee, Knoxville, Tennessee, United States
- ¹¹⁹ University of the Witwatersrand, Johannesburg, South Africa
- ¹²⁰ University of Tokyo, Tokyo, Japan
- ¹²¹ University of Tsukuba, Tsukuba, Japan
- ¹²² University Politehnica of Bucharest, Bucharest, Romania
- ¹²³ Université Clermont Auvergne, CNRS/IN2P3, LPC, Clermont-Ferrand, France
- ¹²⁴ Université de Lyon, CNRS/IN2P3, Institut de Physique des 2 Infinis de Lyon, Lyon, France
- ¹²⁵ Université de Strasbourg, CNRS, IPHC UMR 7178, F-67000 Strasbourg, France, Strasbourg, France
- ¹²⁶ Université Paris-Saclay, Centre d'Etudes de Saclay (CEA), IRFU, Département de Physique Nucléaire (DPhN), Saclay, France
- ¹²⁷ Université Paris-Saclay, CNRS/IN2P3, IJCLab, Orsay, France
- ¹²⁸ Università degli Studi di Foggia, Foggia, Italy
- ¹²⁹ Università del Piemonte Orientale, Vercelli, Italy
- ¹³⁰ Università di Brescia, Brescia, Italy
- ¹³¹ Variable Energy Cyclotron Centre, Homi Bhabha National Institute, Kolkata, India
- ¹³² Warsaw University of Technology, Warsaw, Poland
- ¹³³ Wayne State University, Detroit, Michigan, United States
- ¹³⁴ Westfälische Wilhelms-Universität Münster, Institut für Kernphysik, Münster, Germany
- ¹³⁵ Wigner Research Centre for Physics, Budapest, Hungary
- ¹³⁶ Yale University, New Haven, Connecticut, United States
- ¹³⁷ Yonsei University, Seoul, Republic of Korea
- ¹³⁸ Zentrum für Technologie und Transfer (ZTT), Worms, Germany
- ¹³⁹ Affiliated with an institute covered by a cooperation agreement with CERN
- ¹⁴⁰ Affiliated with an international laboratory covered by a cooperation agreement with CERN.